

Chemolithoautotrophic denitrification intensifies nitrogen loss in Eastern Arabian Sea Shelf waters during sulphidic events

Anil Pratihary^{1,2*}, Gaute Lavik², S.W.A. Naqvi^{1,2,3}, Gayatri Shirodkar¹, Amit Sarkar^{1,4}, Hannah Marchant^{2,5}, Thomas Ohde⁶, Damodar Shenoy¹, Siby Kurian¹, Hema Uskaikar¹, Marcel M. M. Kuypers²

¹Chemical Oceanography Division, CSIR-National Institute of Oceanography, Dona Paula, Goa 403 004, India.

²Department of Biogeochemistry, Max-Planck-Institut für Marine Mikrobiologie, Celsiusstraße 1, D-28359 Bremen, Germany.

³Department of Earth Sciences, Indian Institute of Technology, Kanpur, Uttar Pradesh 208016, India.

⁴Environment and Life sciences Research Centre, P.O. Box 1638, Kuwait Institute for Scientific Research, Salmiya 22017, Kuwait.

⁵MARUM – Center for Marine Environmental Sciences, University of Bremen, 28359 Bremen, Germany

⁶Climate Center, Bavarian Environment Agency, Hans-Högn-Straße 12, D-95030 Hof, Germany

*Corresponding author: Email: apratihary@nio.org, Tel: +91-832-2450639

Abstract:

The Eastern Arabian Sea Shelf i.e. Western Indian Continental Shelf (WICS) – a known biogeochemical hotspot is characterized by monsoonal upwelling, seasonal O₂ deficiency, extremely high N₂O build-up and sulphidic events. The frequency and duration of the sulphidic events have increased over the last two decades, but the impact on pelagic N cycling, the N budget, and N₂O dynamics is poorly constrained. Thus, to address these problems and assess the implications of sulfidic events on WICS biogeochemistry, we carried out physico-chemical measurements, ¹⁵N-labelled incubations and bag incubations on five transects over the shelf during the sulphidic event (September-October) of 2011. We observed a very high rate of sulphide-driven chemolithotrophic denitrification (1885-5825 nM N₂ d⁻¹) in sulphidic, nitrate deplete waters and its potential occurrence in sulfide free, nitrate replete waters (460-3137 nM N₂ d⁻¹) along with high transient N₂O production, and comparably low rates of anammox (0-119 nM N₂ d⁻¹) and DNRA (0-45 nM N d⁻¹). Despite the predominant cloud cover during the monsoon season, we could for the first time show the satellite images of large colloidal sulphur (S⁰) plume associated with the sulphidic events off Western India providing further evidence of extensive sulphide oxidation coupled to denitrification. Sulfide-driven denitrification (mean rate = 2697 nM N₂ d⁻¹) appeared to be the dominant N loss process during the anoxic regime (September-October) replacing the chemoorganotrophic (i.e. heterotrophic) denitrification (342 nM N₂ d⁻¹) that predominates during the preceding suboxic regime (July-August). Overall, the sulfide-driven denitrification rates over the WICS found to be the second highest among the anoxic coastal systems of the world. Furthermore, simultaneous consumption of NO_x⁻ and S²⁻ at a ratio close to the theoretical value in anaerobic incubations of chemocline waters indicated that the sulphide-driven denitrifiers were fixing carbon. The estimated dark C production (0.21 g C m⁻² d⁻¹) due to chemolithoautotrophic denitrification was 18% of the photoautotrophic production and accounted for 15% of the total column productivity. Based on our conservative estimates, chemolithoautotrophic denitrification was responsible for the removal of 0.4 Tg of fixed N and 0.57 Tg of sulphide, and fixation of 0.1 Tg of carbon annually in the shelf waters. Thus, the sulfidic event impacted the biogeochemistry and ecology, and modulated N loss pathways and rates over the WICS. With the expansion and intensification of OMZs induced by global climate change and spreading of dead zones due to increasing anthropogenic activity, chemolithoautotrophic denitrification is likely to become increasingly significant in oceanic N cycle and N budget of shallow marine systems particularly.

Key words: anoxia, sulphide, denitrification, nitrous oxide, autotrophy, shelf, India

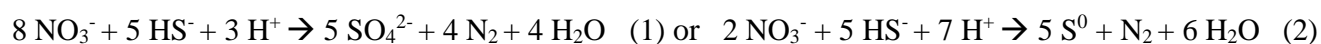
1. Introduction:

Coastal sulphidic events are known to have deleterious impacts on pelagic and benthic life forms, their diversity and ecology, and modify the ecosystem functioning and biogeochemistry often irreversibly, resulting in serious socio-economic consequences and multiple challenges to ecosystem management worldwide (Diaz and Rosenberg, 2008; Breitburg et al., 2018). Anthropogenic activities and global climate change are causing the expansion and intensification of marine oxygen minimum zones (OMZs) (Stramma et al., 2008; Diaz and Rosenberg, 2008; Breitburg et al., 2018; Pitcher et al., 2021) particularly in coastal oceans (Gilbert et al., 2010). More than 500 coastal systems across the world have turned hypoxic ($O_2 < 62 \mu M$) since mid-20th century owing to the above stressors (Diaz and Rosenberg, 2008). However, the biogeochemical, ecological and climatic impact of such deoxygenation is understudied in many coastal and shelf systems.

The bioavailability of fixed inorganic N predominantly controls oceanic primary production (Falkowski, 1997; Tyrrell, 1999), and up to 50% of oceanic N-loss occurs in the four major OMZs *i.e.* the Arabian Sea, the Eastern Tropical North Pacific (ETNP), the Eastern Tropical South Pacific (ETSP) and the Eastern Tropical South Atlantic (ETSA) (Codispoti et al., 2001) via microbially mediated processes such as heterotrophic denitrification (Ward et al., 2009; Dalsgaard et al., 2012) and anaerobic ammonium oxidation *i.e.* anammox (Hammersley et al., 2007; Kuypers et al., 2005; Dalsgaard et al., 2012). In addition, N-transformation processes such as dissimilatory NO_x^- (NO_3^- and/or NO_2^-) reduction to NH_4^+ (DNRA) as well as microaerobic nitrification (NH_4^+ and NO_2^- oxidation) have been shown to be important to N-cycling in some OMZs (Kartal et al., 2007; Lam et al., 2009; Füssel et al., 2012; Bristow et al., 2016).

Apart from the open ocean OMZs, there are numerous seasonal or perennial hypoxic/anoxic coastal and shelf systems, and semi-enclosed basins (Pitcher et al., 2021) which are also significant hotspots of N loss; most notably the Black Sea (Kuypers et al. 2003; Fuchsman et al., 2012), Baltic Sea (Brettar and Rheinheimer, 1991; Bonaglia et al., 2016), Cariaco Basin (Montes et al., 2013; Suter et al., 2021), Golfo Dulce Bay (Dalsgaard et al., 2003), Saanich Inlet (Manning et al. 2010; Michiels et al., 2019), Mariager Fjord (Jensen et al., 2009), Namibian Shelf (Kuypers et al, 2005; Lavik et al., 2009), Peruvian Shelf (Schunk et al., 2013) and Chilean Shelf (Galán et al., 2014). Many of these shallow systems turn sulfidic due to benthic flux of sulphide (defined as $H_2S + HS^- + S^2$). Consequently, where NO_x^- and H_2S co-occur in the water column, microorganisms can couple denitrification to sulfide oxidation (Eq.1). These microorganisms oxidise sulphide to either elemental sulfur or sulfate and are often autotrophs *i.e.* they fix inorganic carbon (Schunk et al., 2013, Callbeck et al., 2021). There is extensive evidence that denitrifying, sulfide oxidizing autotrophs belonging to γ - and ϵ -proteobacteria and particularly the SUP05

clade (Walsh et al., 2009) are abundant and active in sulphidic waters and redoxclines from OMZs worldwide (Cambell et al., 2006; Canfield et al., 2010; Glaubitz et al., 2013; Callbeck et al., 2018; van Vliet et al., 2020), although other species such as *Thiomicrospira spp.*, *Sulfurimonas spp.*, *Candidatus spp.* and *Arcobacter spp.* are also commonly reported in some anoxic coastal systems (Brettar et al., 2006; Glaubitz et al., 2009, 2010; Lavik et al., 2009; Grote et al., 2012, Michiels et al., 2019).



(Burgin and Hamilton, 2008; Lam and Kuypers, 2011)

Chemolithoautotrophic denitrification impacts the biogeochemistry and ecology of coastal and shelf systems in multiple ways. For instance, autotrophic denitrification reportedly removes up to 70% of extraneous N input in the Baltic Sea thereby reducing the possible occurrence of eutrophication (Dalsgaard et al., 2013), furthermore the process is associated with substantial dark CO₂ fixation rates (Taylor et al., 2001; Hügler et al., 2005; Jost et al., 2008). By removing H₂S chemolithotrophic denitrifiers effectively detoxify the water column as sulphide is highly toxic to marine organisms (Levin et al., 2009; Vaquer-Sunyer and Duarte 2010; Lavik et al., 2009). Sulfide-driven denitrification also has the potential to impact emissions of N₂O, a potent green house and ozone depleting gas. Intriguingly, even though many coastal anoxic ecosystems are sources of N₂O, N₂O is generally undetectable or undersaturated in sulphidic bottom waters (Brettar and Rheinheimer, 1991; Schunk et al. 2013, Arevalo-Martinez et al., 2015, 2019, Naqvi et al., 2010). Thus, from biogeochemical, ecological and climatic perspectives, chemolithoautotrophic denitrification has important implications that necessitate comprehensive investigation. With the increasing number of coastal dead zones and frequency of anoxic events on global scale (Diaz and Rosenberg, 2008; Beitburg et al., 2018), it is imperative to understand how their N biogeochemical cycling are likely to respond to such changes.

Western Indian Continental Shelf (WICS), the largest seasonal coastal anoxic system and a biogeochemical hotspot, is one such system which has remarkably transformed from being suboxic (defined throughout as O₂ ≤ 4.4 μM, NO_x⁻ > 0 μM and H₂S = 0 μM (Naqvi et al., 2010)) to anoxic (defined throughout as O₂ = 0 μM, NO_x⁻ = 0 μM and H₂S > 0 μM, or sulfidic/euxinic (Naqvi et al., 2010)). The duration and frequency of the sulphidic events on the WICS have been increasing over last 4 decades due to natural causes and/or increasing anthropogenic activities(i.e. nutrient loading through terrestrial run-off and atmospheric deposition) over the Indian subcontinent (Naqvi et al., 2006, 2009; Gupta et al., 2021). Oxygen deficiency over the shelf sets in with the advent of the Southwest monsoon-induced upwelling in June and intensifies over time, exacerbated by strong thermohaline stratification. During the late southwest monsoon (September-October), the water column becomes NO_x⁻-depleted, and

the bottom waters turn sulphidic, mostly due to sulphide release from the sediments (Pratihary et al., 2014) as documented in similar systems elsewhere (Lavik et al., 2009; Schunk et al., 2013; Galán et al., 2014). Euxinia prevails in the bottom waters until October after which the surface currents reverse and normoxia is re-established. The WICS is probably the only coastal system in the world wherein low oxygen, suboxic and anoxic redox regimes co-occur over outer-shelf, mid-shelf and inner-shelf of the same segment, respectively with such regularity.

The seasonal occurrence of sulphidic events over the WICS was observed as early as 1997 (Naqvi et al. 2000), and since then, NIO's time series observation (CaTS) has shown the frequent occurrence of sulphidic event over the WICS during September to October (Naqvi et al., 2006, 2009). Its increasing frequency is evident from the occurrence of 6 sulphidic events within a decade (1997-2007; Naqvi et al., 2009). Conservative estimates derived from Naqvi et al. (2000) and Shirodkar et al. (2018) show that the area affected by sulphidic event extends from off Kochi (9°N) in the south to off Mumbai (18°N) in the north, and is restricted to up to a mean depth of 35 m over the innershelf thereby occupying an area of ~16,000 Km² which is ~9% of the area of the entire hypoxic zone (i.e. 180,000 Km²) over the WICS. However, the extremity, areal extent and duration of the sulphidic event vary over spatial and annual scales largely due to annual oscillation of the Indian Ocean Dipole (IOD) (Parvathi et al., 2017). For instance, in a few extreme cases (e.g. year 1998, 1999, 2001 and 2003), the sulphidic event lasted from mid-August to October, and the sulphidic zone extended up to the mid-shelf (depth>50 m) with H₂S reaching up to 19 µM, 14 µM, 15 µM and 26 µM H₂S off Mumbai, Goa, Mangalore, and Kochi, respectively (Naqvi et al., 2000, 2009; Shirodkar et al., 2018). However, the impact of sulphidic events on the pelagic biogeochemistry, and in particular N-cycling has remained poorly understood.

Massive N loss has been reported over the WICS during Southwest monsoon season based on δ¹⁵N-NO₃⁻ and δ¹⁸O-NO₃⁻ measurements and ¹⁵N-incubation studies (Naqvi et al., 2006; Bardhan and Naqvi, 2020; Sarkar et al., 2020). Hitherto, denitrification has been reported to be largely the dominant N loss process with anammox and DNRA being mostly insignificant (Sarkar et al., 2020). Interestingly, Sarkar et al. (2020) observed that (1) the mean denitrification rate during a sulphidic event (i.e. year 2009) was >2 fold higher than during non-sulphidic events (i.e. year 2008, 2010), and (2) anammox rates were below detection during the sulphidic event, but were relatively higher during the non-sulphidic conditions. Their study indicated that sulphidic events inhibits anammox and intensifies denitrification in the shelf waters. Furthermore, Naqvi et al. (2006, 2009) observed extremely high N₂O build-up (~0.8 µM) at the oxic-anoxic interface of the shelf water column only during suboxia-anoxia transition period (early September) i.e. when sulphide just starts to build up, which implies that such high N₂O build-up is somehow related to sulphidic event. As the oxygen deficiency over the WICS has intensified over the last 4 decades

leading to extended periods of anoxia (Naqvi et al., 2006, 2009), this can have important implications for the N cycling and budget over the shelf which necessitates a precise mechanistic understanding. We carried out a comprehensive study to understand the coupling of sulphur and nitrogen cycling, and its impact on pathways and rates of N loss, through biogeochemical measurements, shipboard ^{15}N -labeled incubations and bag incubations at some selected stations (which were suboxic or anoxic) at five transects over the WICS during late SW monsoon. We hypothesize that sulphide-driven (chemolithoautotrophic) denitrification becomes the dominant process during late summer monsoon replacing heterotrophic denitrification, intensifies the N loss, and plays a key role in N_2O cycling in the WICS waters.

2. Materials and Methods:

2.1. Study Area:

Our study area is located over the inner continental shelf of Western India (Fig. 1). The WICS occupies an area of 310,000 km^2 , of which the inner shelf comprises ~33% (Mallik, 2008). This region is strongly affected by the monsoons, *i.e.* the biannual reversal of winds and surface currents. Southwest monsoon causes moderate upwelling along the coast during June-September. Due to a unique interplay of physical, hydrographical and biogeochemical changes induced by the southwest monsoon (Naqvi et al., 2006; Parvathi et al., 2017), hypoxia develops over the outershelf and gradually covers the shelf segment between 11° to 18° N (Gupta et al., 2021). Upwelling brings NO_3^- -rich ($>20 \mu\text{M}$) hypoxic water ($\text{O}_2 < 20 \mu\text{M}$) over the shelf which occupies an area of 180,000 km^2 of the shelf area by September. Oxygen progressively falls to $<4 \mu\text{M}$ in July August in the subsurface waters triggering denitrification which exhausts NO_3^- and NO_2^- by mid-September, and the system starts becoming sulphate-reducing (Naqvi et al., 2006; Sarkar et al., 2020). During peak suboxia, (July-August), the water column remains stratified with a 5-10 m thick low saline oxic surface layer overlying a high saline, NO_x^- -rich suboxic layer wherein NO_2^- (up to $8 \mu\text{M}$) and N_2O (200-550 nM) accumulate. As the system transitions from suboxia to anoxia during early September, high N_2O accumulation (up to 765 nM) is often observed at suboxic-anoxic/oxic-anoxic interface (Naqvi et al., 2000). During September to October, O_2 and NO_x^- fall below detection and the subsurface waters turn sulphidic, and become enriched in NH_4^+ and PO_4^{3-} . The intensity of the O_2 deficiency varies spatially along the shelf (north-south) and across the shelf (east-west) at a given time (Naqvi et al., 2006; Gupta et al., 2021), and is also modulated by phase change in IOD (Parvathi et al., 2017). Upwelling starts at off Kerala coast during June and progresses northward and consequently a time lag of ~2 weeks in the development of anoxia has been observed between the southern (off Kerala) and northern (off Goa) part of the shelf. Anoxia at southern transects (off Kerala and Mangalore) is often found to be more intense compared to northern transects (off Mumbai, Goa and Karwar) during September-October. The WICS is the largest natural and seasonal hypoxic coastal system

of the world wherein all three types of redox regimes co-occur across and along the shelf. During November–February, the prevailing northeast monsoon-induced West India Coastal Current (WICC) causes downwelling which reinstates the normoxia that continues till May.

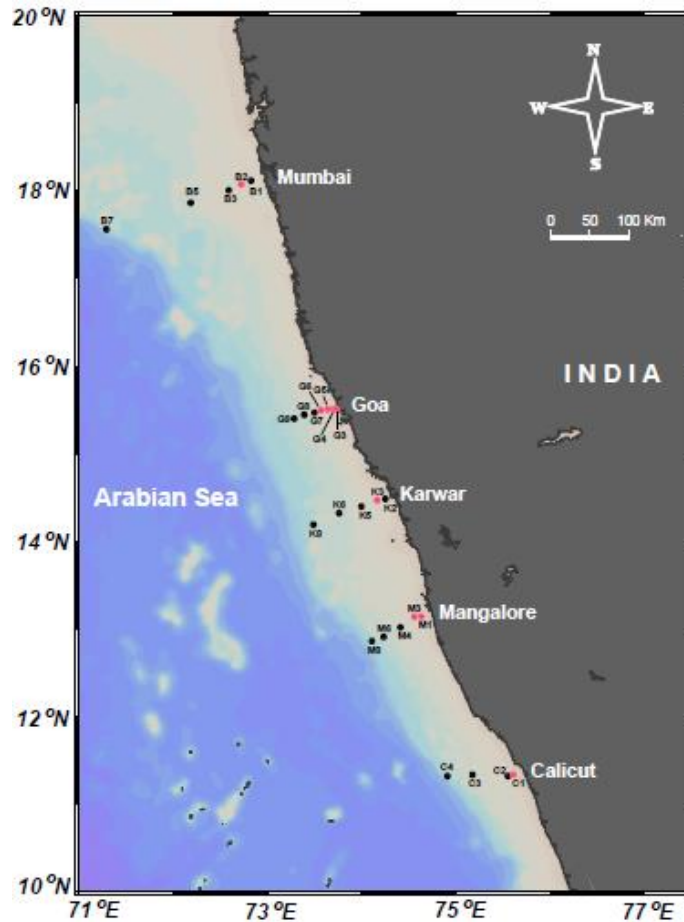


Fig.1. Map of the study area. Dots denote the stations sampled for physical and biogeochemical parameters, and red dots denote the stations where ^{15}N -incubations were carried out.

2.2. Physical and Biogeochemical sample collection:

We covered 5 transects over the WICS (Fig. 1) to carry out our study i.e. off Mumbai (18°N), off Goa (15°N), off Karwar (14°N), off Mangalore (13°N) and off Calicut (11°N) from 15th September to 7th October 2011 onboard *RV Sindhu Sankalp* (SSK024 cruise). Vertical profiles of temperature, salinity and potential density (σ_{θ}) were obtained from a CTD-Rosette sampler (Seabird Electronics). Samples for dissolved O_2 , H_2S , N_2O and nutrients (NO_3^- , NO_2^- , NH_4^+ , PO_4^{3-}) were collected at discrete depths using a CTD Rosette sampler at several stations along these transects. Dissolved O_2 samples were quickly fixed by adding 1 ml each of Winkler's solutions and the oxyhydroxide precipitates were let to settle (Grasshoff et al., 1999). H_2S samples were fixed by addition of a mixed reagent of N, N-dimethyl-*p*-

phenylenediamine dihydrochloride and FeCl_3 (Grasshoff et al., 1999). N_2O samples were immediately poisoned by adding saturated HgCl_2 solution (Naqvi and Noronha, 1991), and nutrient samples were kept at 4°C in the dark until analysis (Grasshoff et al., 1999).

2.3. Satellite imaging of sulphur plume:

The sulphur plumes in the surface water layer were identified in MERIS (Medium Resolution Imaging Spectrometer) and MODIS (Moderate Resolution Imaging Spectroradiometer) images in the expedition period of 15 September to 7 October 2011 as per the methodology of Ohde and Dadou (2018). The corresponding satellite scenes were searched for sulphur events in the study area between Mumbai (18°N) and Calicut (11°N). The method for the identification of sulphur plumes was based on the different optical properties of different water masses in the study area. The sulphur plumes can be clearly distinguished by their special spectral signatures (Suppl. Fig. 1) and milky turquoise color (Fig. 2). They are characterized by very high reflectances in all MERIS bands, especially at the green band of 559.7 nm. The spectral peaks of unaffected offshore and onshore waters, and river plumes are in the blue or green wavelength range depending on the composition of optically active water constituents like chlorophyll-*a*, yellow substances and suspended matter. The offshore waters with low chlorophyll-*a* concentration are characterized by maxima in the MERIS channel of 489.9 nm. The spectra of the onshore waters are influenced by the absorption of chlorophyll-*a* at MERIS bands of 442.6 nm and 664.6 nm. The river plumes with higher concentrations of yellow substances and suspended matter are qualified by their higher spectral peaks compared to the offshore and onshore waters. The river plumes are differentiated from sulphur plumes by their different spectral slopes in the red wavelength range.

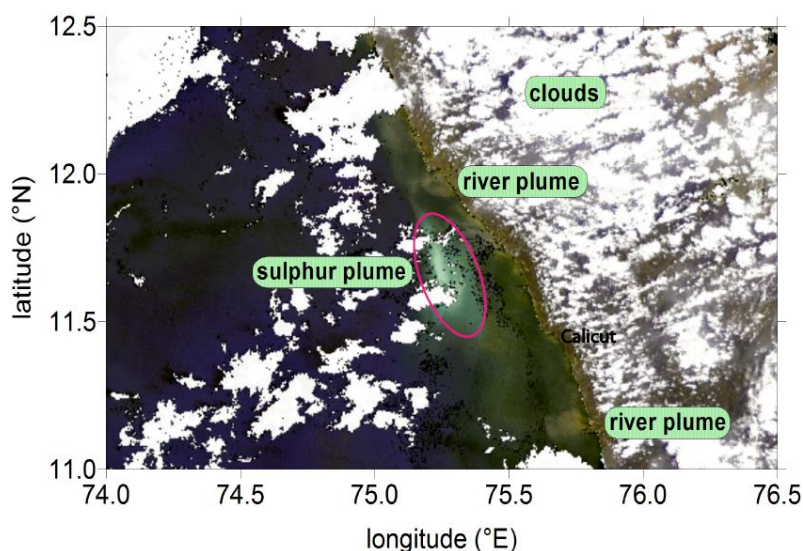


Fig. 2. Satellite-derived image of sulphur plumes (encircled milky turquoise patch) in WICS waters.

2.4. Shipboard ^{15}N labeled incubation:

We carried out a series of shipboard ^{15}N -labelled incubations at stations B2 (off Mumbai), G3, G4, G5 and G6 (off Goa), K3 (off Karwar), M1 and M3 (off Mangalore) and C1 (off Calicut) onboard R/V *Sindhu Sankalp* during September-October 2011 following the methodology by Holtappels et al. (2011). Water samples from selected suboxic/anoxic depths were collected in five 250 ml serum bottle with extreme precaution to avoid O_2 contamination. Thereafter, the water was purged with zero-grade helium (Praxair; 99.999%) for 15 minutes to lower the background $^{28}\text{N}_2$ level, and then spiked with substrates *i.e.* $8\mu\text{M}^{15}\text{NO}_2^-$, $8\mu\text{M}^{15}\text{NO}_2^-+5\mu\text{M Na}_2\text{S}$, $8\mu\text{M}^{15}\text{NO}_2^-+10\mu\text{M Na}_2\text{S}$, $8\mu\text{M}^{15}\text{NO}_2^-+15\mu\text{M Na}_2\text{S}$ and $8\mu\text{M}^{15}\text{NH}_4^+$. The loss of native sulphide due to He purging has been shown to be negligible (~2.5%) (Dalsgaard et al., 2013) as ~97% of the total sulphide pool in seawater is in the form of HS^- (Millero, 1986). The concentrations of the above substrates were chosen so as to mimic their natural concentrations in the WICS waters during seasonal anoxia wherein NO_2^- and NH_4^+ build up to average of ~8 μM each and H_2S builds up to an average of ~5 μM , respectively (Naqvi et al., 2000, 2006, 2009). However, since H_2S level can reach up to ~15 μM or more during extreme anoxic events (Naqvi et al., 2000, Shirodkar et al., 2018), varying concentrations of S^{2-} (*i.e.* 5, 10 and 15 μM) were added along with $^{15}\text{NO}_2^-$ in order to understand the impact of increasing sulphide level on N_2O and N_2 production. ^{15}N substrates were also purged with helium prior to the addition. Details of substrate combination are presented in Table 1. The Na_2S standard solution (50mM) was prepared in helium-purged deionized water inside an N_2 -flushed anoxic chamber. Spiked samples in each bottle were transferred to five 12 ml exetainer vials (Labco Ltd., UK) after sufficient flushing and vials were quickly capped without any head-space. Then the vials were stored in the dark and at temperature close to in-situ temperatures for 48 h. The time points were taken at/close to 0, 12, 24, 36 and 48 h by introducing 2 ml of helium into the vial followed by addition of 100 μL of saturated HgCl_2 . After mixing vigorously, the vials were kept inverted until analysis in order to minimize the exchange of headspace gas with atmosphere through the septum.

Station	Depth (m)	Substrates added in ¹⁵ N-labelled incubation				
		8μM ¹⁵ NO ₂ ⁻	8μM ¹⁵ NO ₂ ⁻ +5μM Na ₂ S	8μM ¹⁵ NO ₂ ⁻ +10μM Na ₂ S	8μM ¹⁵ NO ₂ ⁻ +15μM Na ₂ S	8μM ¹⁵ NH ₄ ⁺
B2	34	√	√	√	√	√
G3	6	√	√	√	√	√
	13	√	√	√	√	√
G4	7	√	√	√	√	√
	15	√	√	√	√	√
G5	14	√	√	√	√	√
	20	√	√	√	√	√
	25	√	√	√	√	√
G6	28	√	√	√	√	√
	34	√	√	√	√	√
K3	20	√	√	√	√	√
	30	√	√	√	√	√
M1	15	√	√	√	√	√
M3	25	√	√	√	√	√
C1	7	√	√	√	√	√
	15	√	√	√	√	√

Table 1. Details of the ¹⁵N-labelled incubations and bag incubations. √ indicates that the incubation with the specified substrate was carried out at that particular depth/station.* indicates that the substrate was not added but allowed to build up over time through pre-incubation.

2.5. Incubation of chemocline water:

A set of bag incubations of water from just below the chemocline (oxic-suboxic or oxic-anoxic interface) depth at a suboxic station (G6) and anoxic station (G5) was also carried out in order to further confirm the coupling of NO_x⁻ reduction to sulphide oxidation (See Table 2). At G6, water from 28 m (0 μM NO₃⁻, 0.29 μM NO₂⁻, 0 μM H₂S) was collected into two 1.5 L Trilaminar gas-tight bags (Pollution measurement corporation, USA). At G5, water from 14 m depth (0 μM NO₃⁻, 0.27 μM NO₂⁻, 0 μM H₂S) was collected into six 1.5 L Trilaminar gas-tight bags. All bags were flushed with helium, and evacuated prior to the filling of water samples. After sampling, the small helium headspace was quickly removed from the bags and the bags were kept at close to in-situ temperature. One bag each from G6 (Bag-A) and G5 (Bag-C) were enriched with 8 μM of ¹⁴NO₂⁻ and one other bag each from G6 (Bag-B) and G5 (Bag-D) were spiked with 8μM of ¹⁴NO₂⁻ and 5 μM Na₂S. The bags were incubated at in-situ temperature for 48 h. No immediate treatment was given to the remaining four bags (Bag E, F, G and H) collected at G5, and they were pre-incubated at temperatures close to in-situ temperatures in order to allow it to turn sulphidic over time. After ~2 weeks of pre-incubation, the enclosed waters were observed to be sulphidic

(~15 μM H_2S) and depleted in NO_x^- (NO_3^- , $\text{NO}_2^- = 0\mu\text{M}$). Then the two bags (Bag-E and Bag-F) were spiked with 16 μM $^{14}\text{NO}_3^-$ and the other two bags (Bag-G and Bag-H) were enriched with 8 μM $^{14}\text{NO}_2^-$ and all the four bags were incubated at in-situ temperature for 48h. Samples from all the bags were collected at every 3-6h interval for NO_3^- , NO_2^- , H_2S and N_2O . NO_2^- was fixed by addition of a mixed reagent of sulphanilamide and N, N-Naphthylidiamine dihydrochloride (Grasshoff et al., 1999), and H_2S samples were immediately fixed as described in the Section 2.2. NO_3^- samples were preserved at 4 $^\circ\text{C}$ and N_2O samples were poisoned by adding 100 μL of saturated HgCl_2 solution.

Bag	Station/Depth	Substrates added	NO_2^- consumption rate ($\mu\text{mol L}^{-1} \text{h}^{-1}$)	S^{2-} consumption rate ($\mu\text{mol L}^{-1} \text{h}^{-1}$)	NO_2^- reduction : S^{2-} oxidation
A	G6, 28 m	8 μM NO_2^-	0.26	--	
B	G6, 28 m	8 μM NO_2^- + 5 μM S^{2-}	0.34	0.19	1.78
C	G5, 14 m	8 μM NO_2^-	0.11	--	
D	G5, 14 m	8 μM NO_2^- + 5 μM S^{2-}	0.21	0.13	1.61
E, F	G5, 14 m	16 μM NO_3^- + 15 μM H_2S^*	0.8	0.56	1.42
G, H	G5, 14 m	8 μM NO_2^- + 15 μM H_2S^*	0.26	0.17	1.52

Table 2. Details of the bag experiments done at G6 and G5, Off Goa. * indicates that the substrate was not added but allowed to build up over time through pre-incubation.

2.6. Analysis:

Dissolved O_2 samples were analyzed by Winkler titration after acidification of oxyhydroxide precipitates (Grasshoff et al., 1999). Nutrient samples were thawed to room temperature, mixed well and analyzed for NO_3^- , NH_4^+ and PO_4^{3-} colorimetrically using a Skalar Autoanalyzer following Grasshoff et al. (1999) within 24h of collection with precisions ± 0.06 , ± 0.01 , ± 0.006 μM , respectively. H_2S and NO_2^- were determined onboard spectrophotometrically following Grasshoff et al. (1999) with precisions ± 0.14 μM and ± 0.02 μM , respectively. N_2O samples were analyzed by a Shimadzu Gas chromatograph equipped with ECD following Multiple Headspace analysis method (McAuliff, 1971) with a precision of 4%.

Headspace samples were analyzed by a GC-IRMS (VG Optima) at the Max Plank Institute for Marine Microbiology (MPIMM), Bremen, Germany for $^{29}\text{N}_2$ ($^{14}\text{N}^{15}\text{N}$), $^{30}\text{N}_2$ ($^{15}\text{N}^{15}\text{N}$), $^{45}\text{N}_2\text{O}$ ($^{14}\text{N}^{15}\text{N}^{16}\text{O}$) and $^{46}\text{N}_2\text{O}$ ($^{15}\text{N}^{15}\text{N}^{16}\text{O}$) following the method given by Holtappels et al. (2011) and Marchant et al. (2018). Prior to N_2O analysis, 25 μL of $^{44}\text{N}_2\text{O}$ standard (99.5%, Air Liquide, Germany) were added to samples to enhance the measurement sensitivity. Calibration for N_2 was done using air as a standard and for N_2O , using the N_2O gas standard. For the determination of DNRA rates, the samples enriched with substrates $^{15}\text{NO}_2^-$ and $^{15}\text{NO}_2^- + \text{S}^{2-}$, were analyzed as follows. First, samples were sufficiently aerated to ensure complete removal of any dissolved $^{15}\text{N}-\text{N}_2$. Then the sample was transferred to a 6 ml exetainer, degassed with Helium and followed by the addition of 5 μM $^{14}\text{NH}_4^+$ and 200 μL of 4 M NaOBr (Warembourg,

1993; Preisler et al., 2007; Jensen et al., 2011). The sample was mixed well and 1 ml of He headspace was created. $^{15}\text{N-N}_2$ produced through the oxidation of $^{15}\text{NH}_4^+$ was analyzed described before.

2.7. Rate Calculation and Statistical analysis:

N deficit was calculated as $N^*=[\text{DIN}-(16\times\text{PO}_4^{3-})]+2.9$ as per Gruber and Sarmiento (2002)

where $\text{DIN} = \text{NO}_3^- + \text{NO}_2^- + \text{NH}_4^+$

The rates of denitrification and anammox were calculated considering the linear increase in excess $^{29}\text{N}_2$ and excess $^{30}\text{N}_2$ in experiments with $^{15}\text{NO}_2^-$ enrichment as per Thamdrup et al. (2006), Holtappels et al. (2011) and Dalsgaard et al. (2012) as given below.

$$N_{2 \text{ anammox}} = {}^{14}\text{N}^{15}\text{N}_{\text{xs}} \times (F_{\text{NH}_4})^{-1} \text{ and}$$

$$N_{2 \text{ denitrification}} = {}^{15}\text{N}^{15}\text{N}_{\text{xs}} \times (F_{\text{NO}_2})^{-2}$$

Where ${}^{14}\text{N}^{15}\text{N}_{\text{xs}}$ is the linear production rate of excess ${}^{14}\text{N}^{15}\text{N}$ i.e. $^{29}\text{N}_2$ with time,

${}^{15}\text{N}^{15}\text{N}_{\text{xs}}$ is the linear production rate of excess ${}^{15}\text{N}^{15}\text{N}$ i.e. $^{30}\text{N}_2$ with time,

F_{NH_4} is the mole fraction of ^{15}N in the NH_4^+ pool in the $^{15}\text{NH}_4^+$ -amended incubations, and

F_{NO_2} is the mole fraction of ^{15}N in the NO_2^- pool in the $^{15}\text{NO}_2^-$ -amended incubations

DNRA rate was calculated from the linear production rate of $^{15}\text{NH}_4^+$ derived from the measured $^{15}\text{N-N}_2$ in the 6 ml exetainer vials as per Lam et al. (2009), Jensen et al. (2011) and De Brabandere et al. (2014) as follows

$$N_{\text{DNRA}} = {}^{14}\text{N}^{15}\text{N}_{\text{xs}} + (2 \times {}^{15}\text{N}^{15}\text{N}_{\text{xs}})$$

By applying LINEST function (MS Excel) on time plot of N_2 , rates of denitrification, anammox and DNRA with standard deviation were calculated and presented in the Table 2 and figures (Fig. 4-6; Suppl. fig. 3-10). As the contributions of anammox and DNRA were very low compared to denitrification, we did not take combined isotope effects taking the co-occurrence of all processes into consideration (Song et al., 2016). To test the significance of variance between the data, ANOVA (MS Excel) was applied and variance was considered significant only where $p < 0.05$.

3. Results:

3.1. Physical and biogeochemical condition over the shelf:

During the study period, the shelf water column was vertically stratified and stratification was more prominent at the northern transects, as reported earlier (Naqvi et al., 2006, 2009, Shirodkar et al., 2018). Briefly, between Mumbai to Mangalore, a warm (27-29°C), low saline (26-33 psu), low dense ($\sigma_\theta = 16-22$

Kg m⁻³), thin (2-7 m) oxic surface layer overlaid cold (22-25°C), high saline (35-36 psu) suboxic/anoxic (0-4 µM O₂) subsurface water (Fig. 4, 5, 6). A relatively weaker vertical stratification was observed at Calicut where a colder (25-26 °C), higher saline (35 psu), denser ($\sigma_\theta = 23$ Kg m⁻³), thin (<1 m) oxic surface layer overlaid slightly colder 23°C and denser ($\sigma_\theta = 23.9$ Kg m⁻³) anoxic (0 µM O₂) subsurface water that had the nearly same salinity as that of the surface layer (Fig. 6d). This indicated that upwelled water surfaced at Calicut (Rao et al., 2008; Gupta et al., 2016) whereas at the northern upwelling was prevented by thermohaline stratification (Naqvi et al., 2006). However, the subsurface layer below the thermocline/pycnocline showed uniform physical characteristics down to the bottom at all stations (Fig. 4, 5, 6) presumably due to small scale vertical mixing induced by internal waves and/or upwelling (Unnikrishnan and Antony, 1990; Shenoi and Antony, 1991).

The intensity of O₂ deficiency varied across the shelf with more intense reducing conditions towards the coast (particularly off Goa, Mangalore and Calicut), leading to the co-occurrence of sulphidic condition (inner-shelf), suboxia (mid-shelf) and hypoxia (outer-shelf) (Fig. 3). On the inner shelf, the thickness of the oxic layer increased progressively from south to north, briefly the oxic layer was very thin (~5 m) at the Goa, Karwar, Mangalore and Calicut, and was comparably thicker (27 m) at the northernmost transect (Mumbai). Accordingly, the volume of the anoxic water mass decreased from south to north. Consequently, strong north-south biogeochemical gradients were observed in terms of O₂, H₂S, N*, N-nutrients, and N₂O (Fig. 7, Suppl. Fig. 2). The intensity of O₂ deficiency increased from north to south which was manifested in suboxia in the northern stations i.e. Mumbai and Karwar except Goa and euxinia in southern stations, which apparently led to significant increase in N* and decrease in N-nutrients from north to south barring the exception at Goa (Fig. 7, Suppl. Fig. 2). Similarly, N₂O showed a decreasing trend from north to south with only an exceptional high at Mangalore (Suppl. Fig.2).

The prevailing biogeochemical conditions in the bottom water clearly reflected 3 types of redox regimes over the WICS; (1) hypoxic bottom waters with measurable NO₃⁻, low NO₂⁻ and low N₂O concentrations with a moderate to low N* signal i.e. at stations over mid- and outershelf, (2) suboxic bottom waters with low NO₃⁻ but high NO₂⁻ and N₂O concentrations combined with a substantial N* signal i.e. at B2, G6, K3 and M3, (3) anoxic bottom waters depleted in NO₃⁻ and NO₂⁻ with detectable sulphide (>0.1 µM) and high NH₄⁺ i.e. at G3, G4, G5, M1 and C1 (Fig. 3, 4, 5, 6). On the Mumbai, Karwar and Mangalore transects, suboxia developed towards the coast and NO₃⁻ dropped substantially while NO₂⁻ accumulated concomitant with an increase in N* (stations B1-B3, K2-K3, M1-M6) (Fig. 3), and except at M1, sulphide was not detected at any of these stations. The Goa transect exhibited all three conditions, with hypoxic conditions on the outershelf (G8 and G9), suboxic conditions with high NO₂⁻ concentrations and N₂O accumulation on the mid shelf (G6-G7), and anoxic (sulphidic) conditions on the inner shelf (G3-

G5). At Calicut, the bottom waters at stations C1 and C2 were sulphidic and depleted with NO_3^- and NO_2^- . At the station closest to the shore (C1), O_2 fell below detection at 7m water depth and H_2S was detectable just below the oxic-anoxic interface, reaching concentrations of $6 \mu\text{M}$ in the bottom water (Fig. 6).

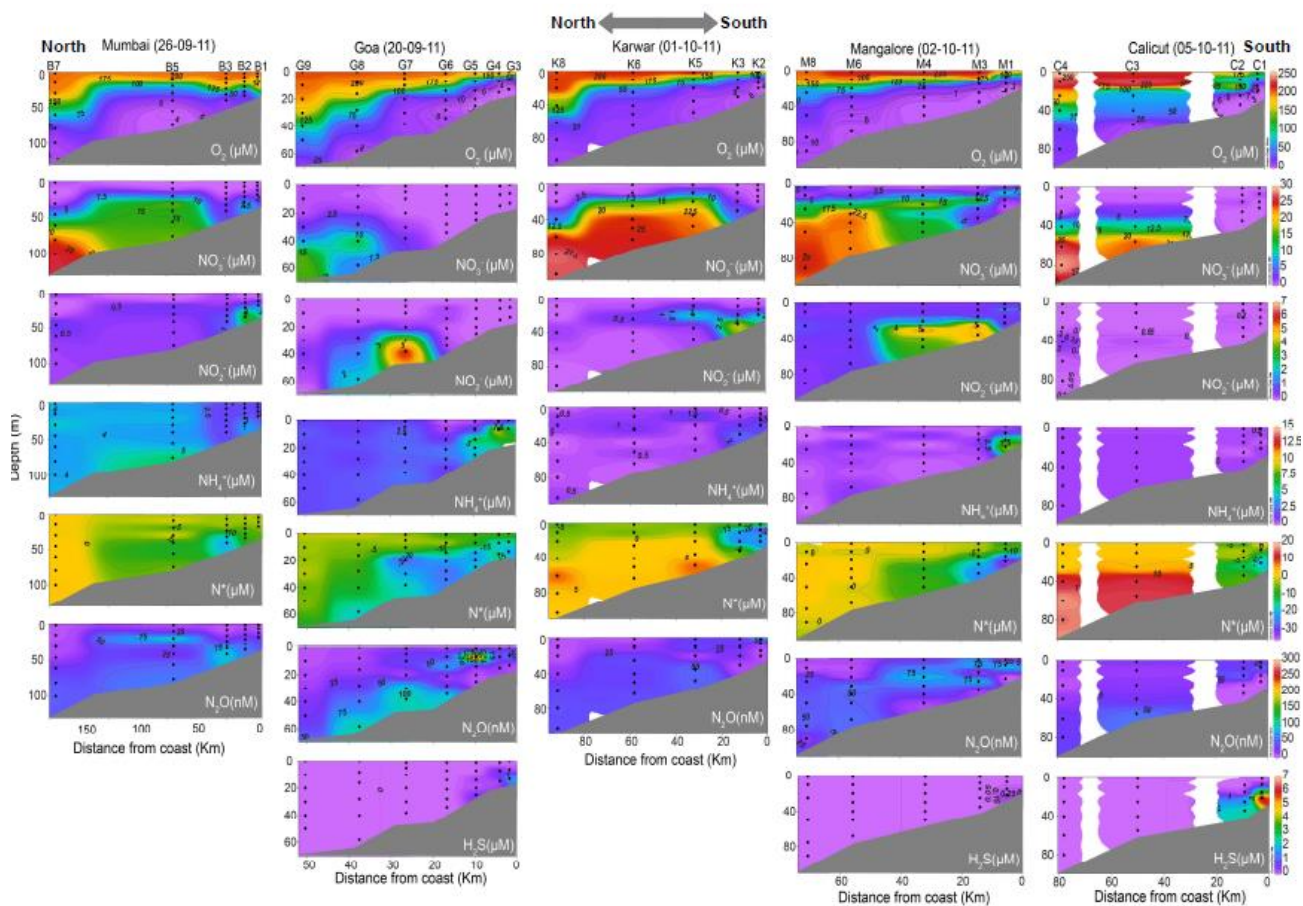


Fig.3. Cross-shelf variation of the biogeochemical parameters along the five transects off the Western Indian shelf. Some of the data from off Mumbai, Goa, Mangalore and Calicut transects are taken from Bardhan and Naqvi (2020).

3.2. Denitrification, N_2O , DNRA and anammox rates in the presence and absence of sulphide

3.2.1. Mumbai transect:

Incubations were carried out in the suboxic bottom water (34 m) at the station B2. The denitrification rate was moderate ($261 \text{ nmol N}_2 \text{ L}^{-1} \text{ d}^{-1}$) in comparison to other stations (Fig. 4; Table 3) and was orders of magnitude higher than anammox rate. Furthermore, a transient accumulation of $^{15}\text{N-N}_2\text{O}$ was observed in the incubation ($^{45}\text{N}_2\text{O}$ and $^{46}\text{N}_2\text{O}$) (Suppl. fig. 3a). Upon addition of sulphide, denitrification rates increased >2 fold (Table 3; Fig. 4), and the transient accumulation of N_2O was substantially higher (Suppl. fig. 3a). Furthermore, the addition of sulphide led to the occurrence of DNRA (Fig. 4; Table 3), although at rates orders of magnitude lower than denitrification.

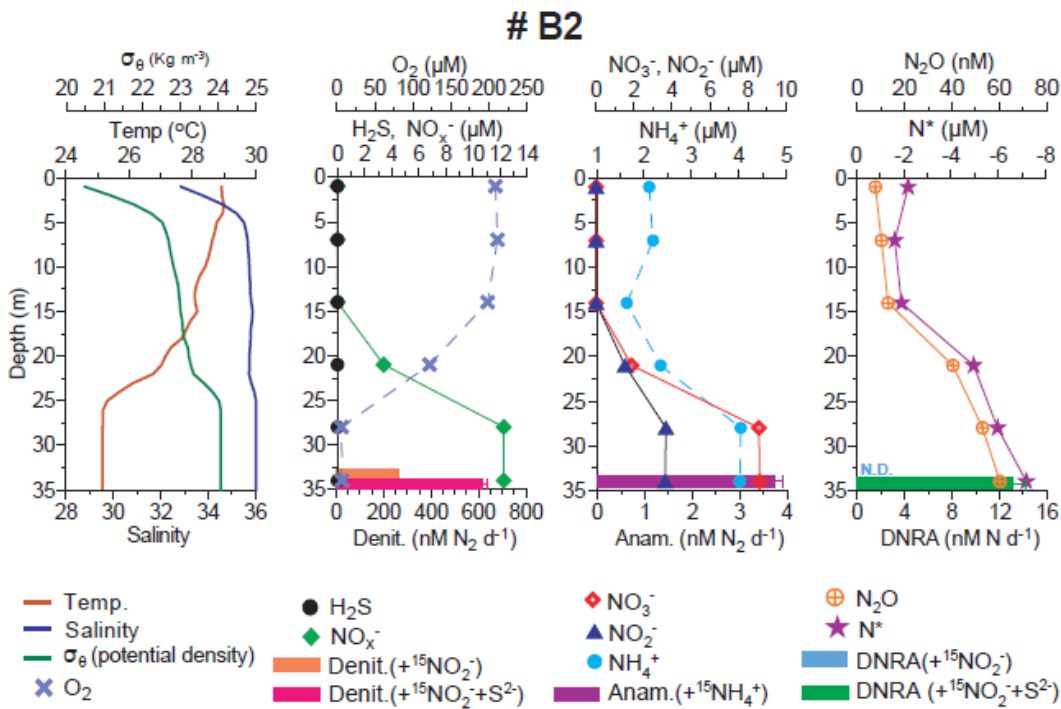


Fig.4. Physico-chemical condition and N transformation rates at station B2, off Mumbai. Denit.: Denitrification, Anam.: anammox, N.D.: not detected.

3.2.2. Goa transect:

At the stations with measurable sulphide on the Goa transect (G3, G4 and G5), incubations were carried out in the sulphidic bottom waters and just below the NO_x^- - H_2S chemocline, where NO_2^- concentrations peaked and sulphide dropped below detection. At G5, incubations were also carried out at an additional depth located between the bottom water and the chemocline (Fig. 5). Denitrification was the dominant process at all depths (221-2921 $nM N_2 d^{-1}$), followed by DNRA (5.3-45 $nM N d^{-1}$) and anammox (0-41 $nM N_2 d^{-1}$) (Fig. 5; Table 3). At the depth below the chemocline of G3 (6 m), G4 (7 m) and G5 (14 m) or in the G3 bottom water (13 m), sulphide addition had no significant effect on denitrification rates ($p=0.79$) but did stimulate rates in the bottom water of G4 (15 m) and G5 (20 m and 25 m) significantly ($p=0.02$). Sulphide addition significantly stimulated DNRA rates in all incubations ($p=0.002$) with the exception of the oxic-anoxic interface at G3 (6 m) and G5 bottom water (25 m) ($p=0.85$). At G6, where no NO_3^- or sulphide was measurable in the water column, incubations were carried out below the oxic-suboxic interface where nitrite was undetectable (28 m) and in the bottom water (34 m) where NO_2^- peaked. The denitrification rate ranged from 104 $nM N_2 d^{-1}$ at 28 m and 901 $nM N_2 d^{-1}$ at 34 m. No DNRA was detected at 28m, but a rate of 7.2 $nM N d^{-1}$ could be detected at 34 m, which was the lowest DNRA rate measured during this study. Similarly,

anammox rates were very low at 28m (1.5 nM N₂ d⁻¹) and rose to 27 nM N₂ d⁻¹ at 35m. The addition of sulphide led to an increase in denitrification rates by more than an order of magnitude at 28 m but by ~3 fold at 34 m. Sulphide addition led to measureable DNRA at 28 m and doubled the rate at 35 m. At all the stations on the Goa transect, a transient production of ¹⁵N-N₂O was observed and with sulphide addition, this intermediate ¹⁵N- N₂O production increased substantially at all stations off Goa (Suppl. fig. 3b, 4, 5, 6 and 7).

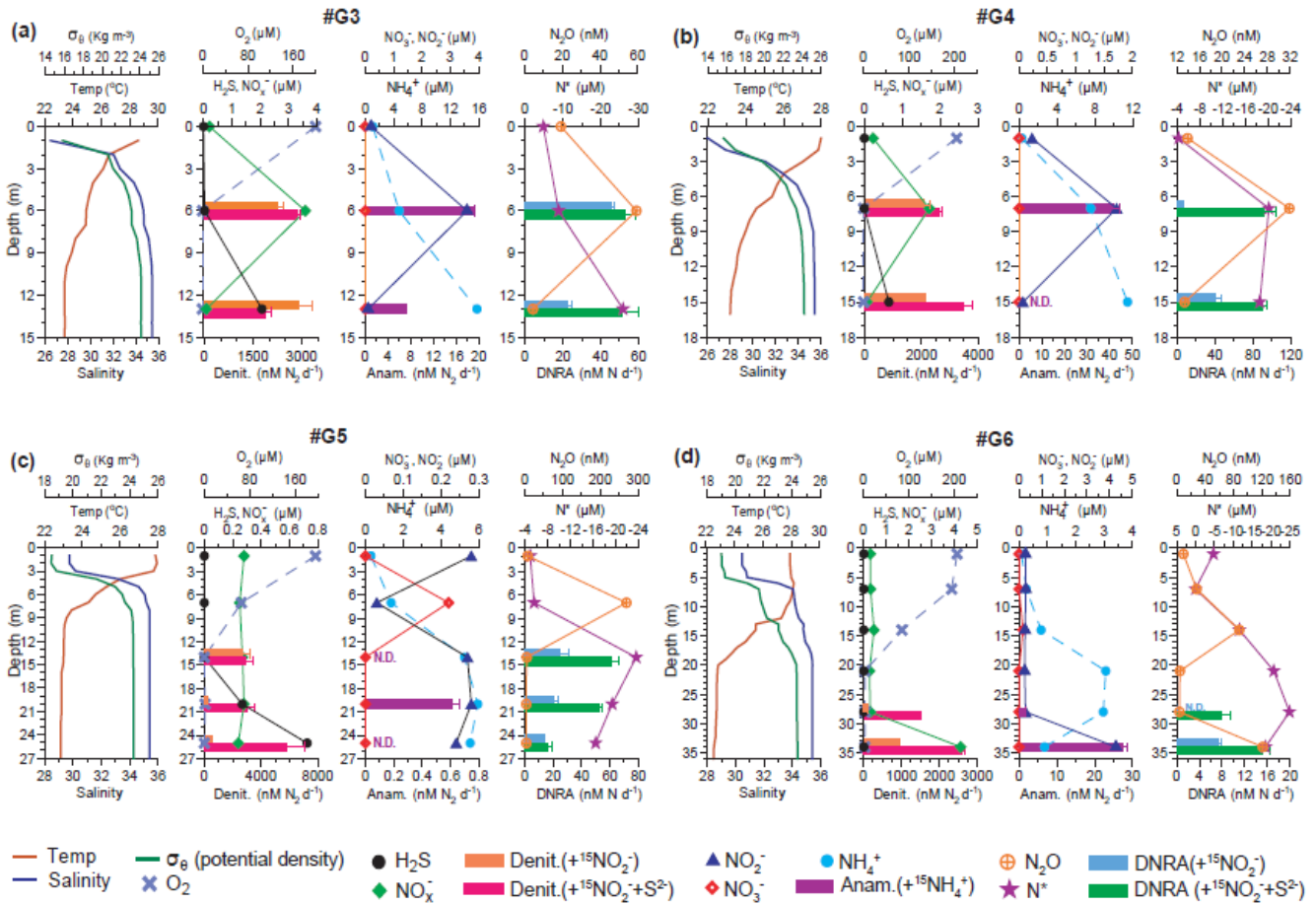


Fig. 5. Physico-chemical condition and N transformation rates at stations G3, G4, G5 and G6, off Goa. Denit.: Denitrification, Anam.: anammox, N.D.: not detected.

3.2.3. Karwar transect:

Incubations were carried out at station K3 on the Karwar transect at just below the oxic-suboxic interface (20 m) and in the bottom water (30 m). At K3, bottom water was non-sulphidic with high NO_x^- and NH_4^+ concentrations. Denitrification was the dominant process at both the depths (264-408 nM N₂ d⁻¹) followed by anammox (6.5-33 nM N₂ d⁻¹) and DNRA (8-30 nM N d⁻¹) (Fig. 6a; Table 3). Upon the sulphide addition, denitrification was stimulated by 7.6 fold at 20 m and 1.7 fold at 30 m. Sulphide addition led to 4.5 fold increase in DNRA rate at 20 m but no stimulation was observed at 30

m. Transient accumulation of N_2O was observed during the incubation although not very prominently at 20m. However, sulphide addition significantly stimulated N_2O accumulation at both the depths (Suppl. fig. 8).

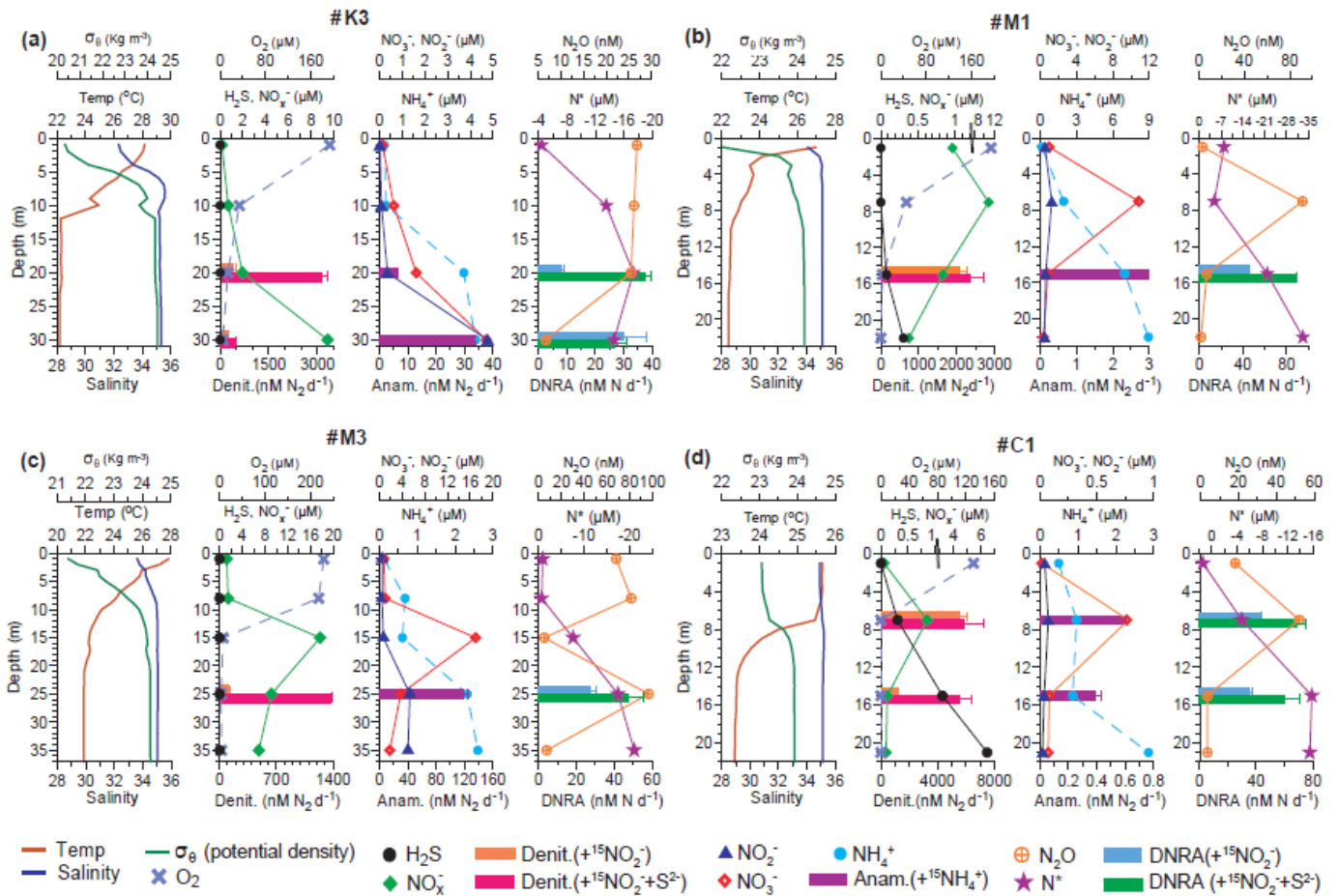


Fig.6. Physico-chemical condition and N transformation rates at stations K3 (off Karwar), M1 and M3 (off Mangalore, and C1 (off Calicut). Denit.: Denitrification, Anam.: anammox, N.D.: not detected.

3.2.4. Mangalore transect:

Incubations on the Mangalore transect were carried out at two stations (M1 and M3). At station M1, where the bottom water was depleted in NO_3^- and NO_2^- but H_2S was detectable, incubations were carried out at just below the NO_x^- - H_2S chemocline (15 m). The denitrification rate ($2079 \text{ nM } N_2 \text{ d}^{-1}$) was much higher than the DNRA and anammox rate (Fig. 6b, Table 3) and was associated with a transient production of N_2O (Suppl. fig. 9a). Upon addition of sulphide, there was no significant increase in denitrification rate, but there was a higher transient production of N_2O and DNRA rates doubled. Station M3 still had measureable NO_3^- and NO_2^- in the bottom water but no H_2S (Fig. 6c) and incubations were carried out at 25 m. In incubations without added sulphide, the denitrification rate

(114 nM N₂ d⁻¹) was nearly same as anammox rate (119 nM N₂ d⁻¹) but higher than DNRA (27 nM Nd⁻¹) and a transient peak of N₂O accumulation was observed (Suppl. fig. 9b). The addition of sulphide caused denitrification to increase by an order of magnitude (1358 nM N₂ d⁻¹), DNRA to double and led to a steady accumulation of N₂O.

Station	Depth (m)	Denitrification (nmol N ₂ L ⁻¹ d ⁻¹)	Denitrification with S ²⁻ (nmol N ₂ L ⁻¹ d ⁻¹)	Anammox (nmol N ₂ L ⁻¹ d ⁻¹)	DNRA (nmol N L ⁻¹ d ⁻¹)	DNRA with S ²⁻ (nmol N L ⁻¹ d ⁻¹)
B2	34	261 (±2.8)	615 (±19)	3.7 (±0.18)	n.d.	14 (±1.1)
G3	6	2242 (±184)	2860 (±114)	18.8 (±0.45)	45 (±1.4)	53 (±5.5)
	13	2921 (±388)	1885 (±197)	7.1 (±0.22)	22 (±1.9)	51 (±8.7)
G4	7	2106 (±165)	2608 (±100)	41 (±2.9)	5.3 (±0.39)	91 (±12)
	15	2120 (±37)	3455 (±359)	n.d.	40 (±6.4)	90 (±3.8)
G5	14	2646 (±551)	2880 (±520)	n.d.	24 (±6.4)	60 (±5.3)
	20	221 (±6.8)	2990 (±515)	0.61 (±0.04)	19 (±3.2)	52 (±2.1)
	25	544 (±78)	3081 (±470)	n.d.	13 (±0.13)	15 (±3)
G6	28	104 (±18)	1495 (±14)	1.5 (±0.08)	n.d.	7.9 (±1.5)
	34	901 (±50)	2615 (±45)	27 (±1.5)	7.2 (±0.75)	15 (±1.4)
K3	20	408 (±63)	3137 (±187)	6.5 (±0.17)	8.1 (±0.91)	37 (±2.2)
	30	264 (±5.5)	460 (±23)	33 (±0.6)	30 (±7.6)	26 (±4.3)
M1	15	2079 (±192)	2365 (±350)	2.9 (±0.02)	44 (±2.1)	89 (±0.34)
M3	25	114 (±7.9)	1358 (±26)	119 (±5.4)	27 (±2.8)	47 (±7.8)
C1	7	5573 (±531)	5825 (±1363)	0.58 (±0.02)	40 (±1.4)	68 (±6.1)
	15	1087 (±104)	5518 (±817)	0.38 (±0.04)	35 (±2.6)	59 (±11)

Table 3. N transformation rates with SD (in parenthesis) in the WICS waters as determined through ¹⁵N-incubations.

3.2.5. Calicut transect:

The incubations on the Calicut transect were carried out at station C1, at a depth just below the oxic-anoxic interface (7 m) and in the bottom water (15 m) which were NO_x⁻ depleted, sulphidic and had NH₄⁺ concentrations up to 2.5 μM (Fig. 6d). At the oxic-anoxic interface (7 m), the denitrification rate was 5825 nM N₂ d⁻¹, which was the highest rate measured at any station with no added sulphide in the incubation (Table 3; Fig. 6d). The DNRA rate (40 nM N d⁻¹) was similar to other stations (Table 2) and anammox rates were extremely low (0.58 nM N₂ d⁻¹). At 15 m, denitrification still dominated over DNRA and anammox but the rates were 5 times lower than that at 7 m (Table 3). Upon addition of sulphide, no discernible increase was observed in the denitrification rate at 7 m, but it increased 5 fold

to 5518 nM N_2 d^{-1} at 15 m, and 2 fold increases in DNRA rates at both the depths. Sulphide addition also led to higher transient production of N_2O at both the depths (Suppl. fig. 10).

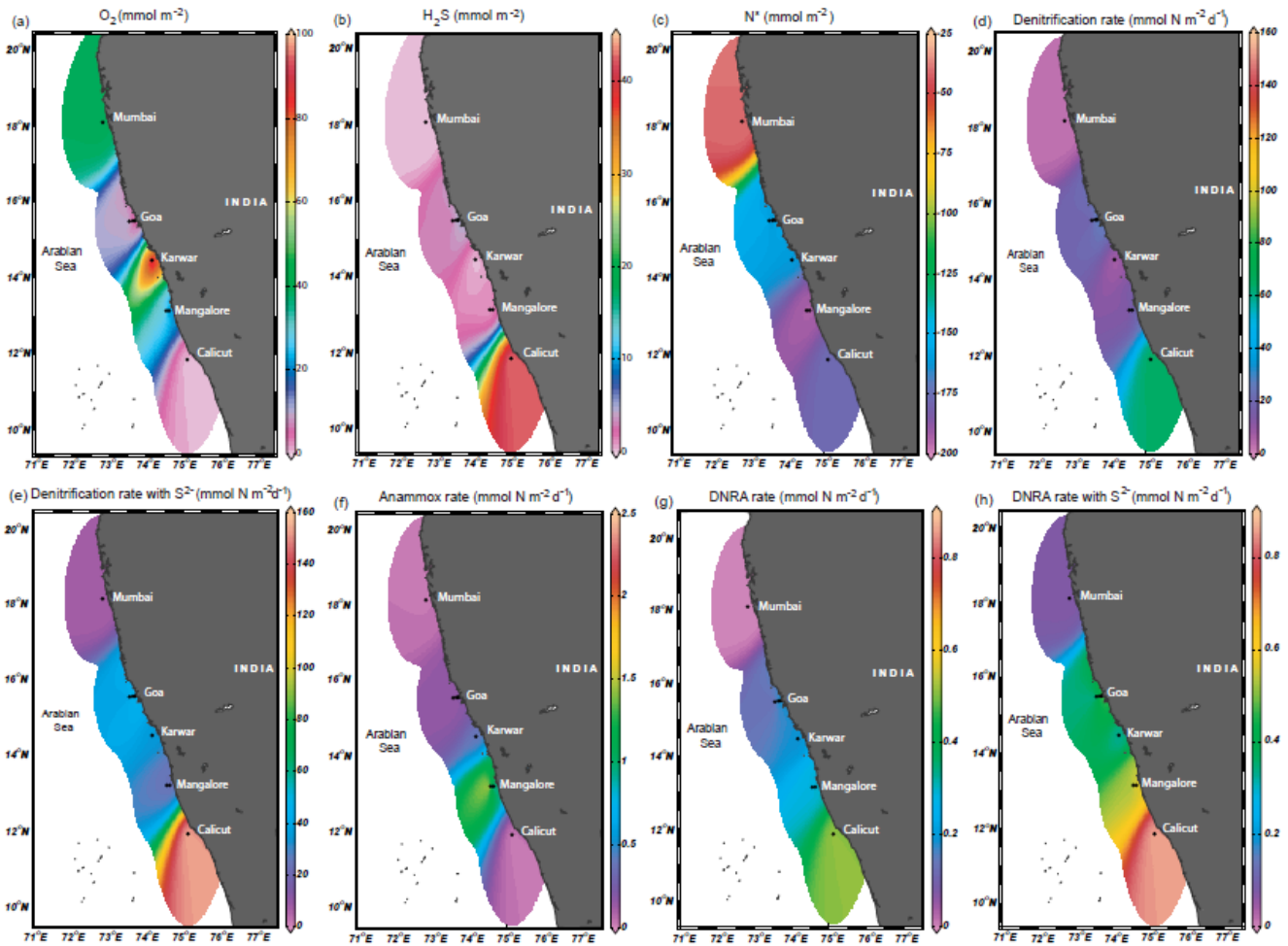


Fig.7. Spatial variability of depth-integrated O_2 , H_2S , N -deficit, denitrification, anammox and DNRA rates in the subsurface waters of WICS during the study period.

3.3. Variability of N loss/transformation rates along the shelf:

Depth-integrated denitrification, anammox and DNRA rates exhibited significant variability from north to south over the shelf (Fig. 7) in response to variability in O_2 deficiency and N -nutrient availability. The denitrification rate showed an overall increase from Mumbai to Calicut, apart from at Karwar, and there was a trend towards increasing denitrification rate upon S^{2-} addition from north to south with higher rates (with the exception of a decrease at Mangalore). No regular trend in the anammox rate was observed from north to south; rather it increased from north to a maximum at Mangalore and further decreased towards south. A clear increasing trend in the DNRA rate was noticed from north to south, furthermore, with S^{2-} addition the DNRA rates increased but the trend remained the same.

3.4. NO_x^- reduction, sulphide oxidation, and N_2O build-up in the bag incubations:

Bag incubation of chemocline waters from stations G5 (14 m) and G6 (28 m) showed similar results. In the Bags A-D, NO_2^- decreased linearly over time and a transient accumulation of N_2O was observed (Fig. 8). Relative to the incubations with only added NO_2^- (Bag A and C), in the incubations with added $\text{NO}_2^- + \text{S}^{2-}$ (Bag B and D), NO_2^- consumption rates (Table 2) were higher and N_2O accumulated faster and to higher concentrations until net consumption began (Fig. 8). NO_2^- and sulphide were both consumed linearly in a ratio of 1.61-1.78 (Table 3). Similar pattern of NO_2^- reduction, S^{2-} oxidation and N_2O production/consumption at both G5 and G6 indicated that the results could be replicated at different stations. In the Bags E and F (native sulphide + NO_3^-), no appreciable change in NO_3^- and H_2S concentrations occurred for the first 6h, after which a rapid simultaneous decrease in the concentrations of both occurred until 24h (Fig. 8) at a ratio of 1.42 (Table 3). NO_2^- accumulated after 6h and peaked up to 13 μM at 24 h followed by a steady decrease. A rise in N_2O was observed from 0h until 24h after which concentrations increased steeply, peaking to 125 nM at 42 h and decreasing rapidly afterwards. There was no statistically significant variance in the experimental results between the two bags ($n=9$, $p>0.7$; ANOVA) indicating good reproducibility. In the Bags G and H (native sulphide + NO_2^-), NO_2^- and H_2S decreased simultaneously at a ratio of 1.52 (Table 3) and N_2O started increasing steadily from 0h (Fig. 8). NO_2^- was undetectable after 30 h but 9-12 μM of H_2S remained at the end of the experiment. A sharp increase in N_2O concentrations was observed after 12 h, peaking up to 472 nM at 18h followed by a rapid decrease. Concentration change patterns between in the two bags did not vary significantly ($n=9$, $p>0.2$; ANOVA) implying a good replication of the results. The mean consumption rates of NO_2^- and S^{2-} derived from the Bags B, D, G and H were $0.27 \pm 0.07 \mu\text{mol N L}^{-1} \text{h}^{-1}$ and $0.16 \pm 0.03 \mu\text{mol L}^{-1} \text{h}^{-1}$, respectively, and the mean consumption ratio of NO_2^- to S^{2-} was 1.58. Overall, the bag incubation of the chemocline waters from both G6 and G5 showed simultaneous NO_x^- reduction and S^{2-} oxidation along with transient N_2O production, indicating that the NO_x^- reduction to N_2 was coupled to the oxidation of native or added sulphide, and that both NO_x^- reduction and N_2O production are stimulated by increasing sulphide level.

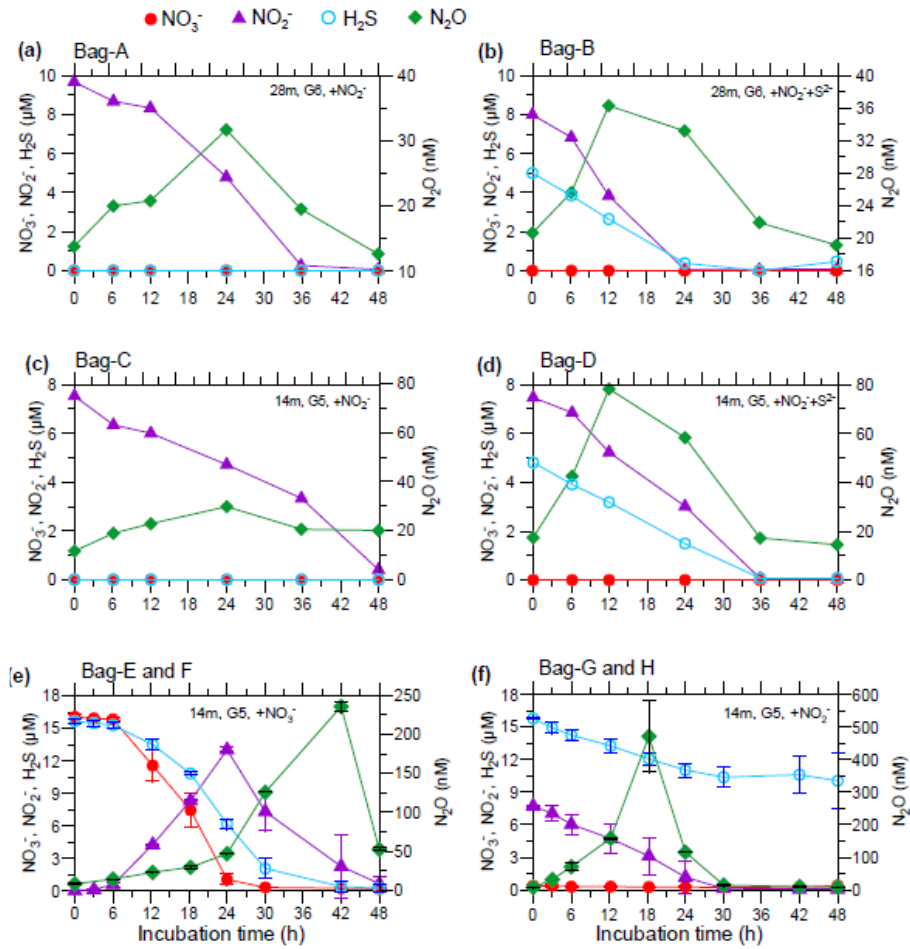


Fig.8. Incubation of water from the suboxic-anoxic interface at G6 (a) with added NO_2^- and (b) with added $\text{NO}_2^- + \text{S}^{2-}$; incubation of water from the suboxic-anoxic interface at G5 (c) with added NO_2^- and (d) with added $\text{NO}_2^- + \text{S}^{2-}$; incubation of water from suboxic-anoxic interface at G5 after ~ 2 weeks of pre-incubation (e) mean results of bag E and F spiked with NO_3^- (f) mean results of bag G and H spiked with NO_2^- .

4. Discussion:

4.1. Signatures of N-loss, and build-up of N_2O and H_2S

During the study period, the prevailing biogeochemical characteristics of the WICS waters were suboxic at stations B2, G6, K3 and M3, and anoxia at stations G3, G4, G5, M1 and C1, since the subsurface waters at the former stations were sulphide-free and NO_x^- -replete whereas the subsurface waters at the latter stations were sulphidic and NO_x^- -depleted (Fig. 4, 5, 6). The intensity of O_2 deficiency, OMZ thickness, NO_x^- concentrations and N^* indicated N-loss which increased southward. Such observations are in line with the patterns previously observed during the southwest monsoon season (Naqvi et al., 2006; Bardhan and Naqvi, 2020; Sarkar et al., 2020). At the stations closest to the coast over Goa, Mangalore and Calicut transect i.e. G3, G4, G5, M1 and C1, the bottom waters were nearly depleted in NO_x^- , and exhibited higher N^* values and detectable sulphide (Fig. 5, 6) compared to the stations farther from the coast (Fig. 3). In contrast, at the stations closest to the coast on the Mumbai and Karwar

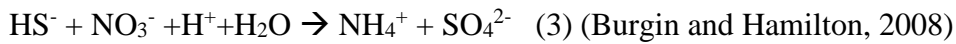
transects (B2 and K3), and G6 and M3, there was a prominent NO_2^- accumulation and relatively lower N^* (Fig.4, 5, 6). Together these results indicate that denitrification was occurring at the above four stations, but was less advanced than at the sulphidic stations. Interestingly, the pattern of N_2O accumulation differed between the sulphidic and non-sulphidic stations. At the non-sulphidic stations (e.g. B2, G6, K3, M3), the highest N_2O concentration was observed within the OMZ core and lower N_2O was observed at the oxic-anoxic interface (Fig. 4, 5d, 6c). In contrast, at the sulphidic stations (e.g. G3, G4, G5, M1, and C1), the opposite was true *i.e.* the N_2O peak was observed at or just above the oxic-anoxic interface, and was depleted within the core of OMZ (Fig. 5a-c, 6b, d). At the sulphidic stations (G3, G4, G5, M1 and C1), a clear overlapping of NO_x^- and H_2S profiles was conspicuous wherein substantial NO_x^- concentration (0.27-3.6 μM) was detected at the oxic-anoxic interface, which decreased further down to the bottom (Fig. 5, 6). Even the near bottom sulphidic water contained some traces of NO_x^- (0.1-0.86 μM) which clearly indicated the mixing of NO_x^- -replete suboxic water with underlying sulphidic water. Co-existence of NO_x^- and H_2S occurred possibly due to (1) the small scale vertical mixing via turbulent motions induced by internal waves (Unnikrishnan and Antony, 1990; Shenoi and Antony, 1991) as also observed in the Baltic Sea (Hannig et al., 2007; Dalsgaard et al., 2013) and/or (2) the vertical movement of water caused by upwelling (Unnikrishnan and Antony, 1990). This was substantiated by the uniformity of σ_θ from the oxic-anoxic interface to the bottom at these stations (Fig. 5a, b, c; Fig. 6b, d). The thickness of the mixing zone of NO_x^- and H_2S *i.e.* *substrate mixing zone* (SMZ) varied from 7 to 15m at the sulphidic stations with an average of 11 m.

4.2. Impact of sulphide on anammox and DNRA rates:

Anammox was detected at most sampled stations and depths, with a maximum rate of 119 $\text{nM N}_2 \text{d}^{-1}$ at station M3 (Fig. 6c; Table 3). Previously, Naqvi et al. (2006) suggested a high potential for anammox activity in the shelf waters during seasonal anoxia as the benthic-released NH_4^+ (Pratihary et al., 2014) can enter the overlying NO_2^- -rich bottom water. We observed higher anammox rates *i.e.* 1.5-119 $\text{nM N}_2 \text{d}^{-1}$ at the non-sulphidic stations compared to the sulfidic stations where anammox occurred at 0-41 $\text{nM N}_2 \text{d}^{-1}$. Particularly, in the sulphidic bottom waters, anammox rates were extremely low (0-7 $\text{nM N}_2 \text{d}^{-1}$) often being below detection. Our observation is consistent with Sarkar et al. (2020) who previously reported higher average anammox rates in the shelf waters during suboxic (non-sulfidic) events (70 $\text{nM N}_2 \text{d}^{-1}$) compared to sulphidic events wherein anammox was below detection. These observations indicate that the sulfidic event apparently suppressed the anammox activity in the shelf waters as also observed in other coastal systems (Dalsgaard et al., 2003; Jensen et al., 2008). Thus, we believe that anammox was possibly more prominent during the early phase of seasonal anoxia over the shelf (July-August) owing to

sufficient NO_x^- availability and absence of sulphide, and with the intensification of anoxia, it decreased substantially often being undetectable.

Accumulation of $^{15}\text{NH}_4^+$ in the $^{15}\text{NO}_2^-$ labeled incubations suggested that a part of the added NO_2^- was reduced to NH_4^+ via DNRA. Like anammox, DNRA was detected at most depths and stations at rates 0-45 nM N d^{-1} , almost in the similar range of anammox rates. Particularly, it occurred at relatively higher rates (5.3-45 nM N d^{-1}) at the sulphidic depths compared to non-sulphidic depths (0-30 nM N d^{-1}) ($p=0.02$). Moreover, the addition of sulphide to incubations led to a significant increase (1.17-17 times) in DNRA rates at 13 out of 16 depths tested. In fact, at B2 (34 m), and G6 (28 m), DNRA was detectable only after addition of sulphide. Sarkar et al. (2020) also reported higher DNRA rates in the shelf waters during anoxia than during suboxia wherein DNRA was mostly undetectable. These observations suggested that the DNRA in the shelf waters was largely sulphide-driven (Eq. 3) as also observed in other coastal marine systems (Hannig et al., 2007; Bernard et al., 2015; Bonaglia et al., 2016).



4.3. Evidence for sulphide-driven autotrophic denitrification:

By and large, denitrification was found to be the dominant process at all stations with the only exception at M3 (25 m) where it was marginally exceeded by the anammox rate (Table 3). Previously, Sarkar et al. (2020) have reported higher denitrification rates (mean = 3.2 $\mu\text{mol N}_2 \text{ L}^{-1} \text{ d}^{-1}$) in the WICS during a sulphidic year (2009) than during two non-sulphidic years (mean = 1.53 $\mu\text{mol N}_2 \text{ L}^{-1} \text{ d}^{-1}$; 2008 and 2010), and they hypothesized that the higher denitrification rate during anoxia was due to the effect of sulfide. We observed that denitrification rates were generally higher in water sampled from sulfidic stations and depths (G3, G4, G5, M1 and C1; 221-5773 $\text{nmol N}_2 \text{ L}^{-1} \text{ d}^{-1}$) than in those from non-sulfidic stations and depths (B2, G6, K3 and M3; 104-901 $\text{nmol N}_2 \text{ L}^{-1} \text{ d}^{-1}$) (Table 3). Furthermore, denitrification rates increased significantly (1.6-14 times) upon sulfide addition in 10 out of 16 depths ($p=0.006$), and the magnitude by which they increased appeared to be related to the in-situ sulphide concentrations, i.e. there was a stronger increase in denitrification rates upon sulphide addition in samples from the non-sulfidic waters (1.7-14 times), compared to those from already sulfidic waters (0.65-13 times). In contrast, just below chemocline of the sulphidic stations, no significant increase in denitrification rate (1.05-1.28 times) was observed with added $^{15}\text{NO}_2^- + \text{S}^{2-}$ compared to that with only $^{15}\text{NO}_2^-$ addition ($p=0.69$). This indicated that the growth of denitrifiers at these stations was possibly already near saturation with respect to the native sulphide level which led to a marginal enhancement in the denitrification rates upon extra sulphide addition. Moreover, the bag incubations of the chemocline waters from both suboxic and anoxic stations (Fig.

8) showed that the NO_x^- reduction and transient N_2O production were coupled to sulphide oxidation, and were stimulated by increasing sulphide level, as also observed elsewhere (Jensen et al., 2009; Dalsgaard et al., 2013; Galán et al., 2014).

We also observed the elemental sulphur plumes adjacent to the reported sulphidic waters of WICS, which are also indicative of chemolithotrophic sulphide oxidation coupled with denitrification, as observed in other euxinic coastal systems (Schunk et al., 2013; Callbeck et al., 2018; Ohde, 2018; Ohde and Dadou, 2018). However, detection of S^0 plume only at the southern transect (near Calicut) rather than at the northern transects indicated that the upwelling of chemolithotrophically produced S^0 in the subsurface waters is prevented at the latter transects. During South-west monsoon, the upwelled water is known to surface off Southwest Indian coast (Rao et al., 2008; Gupta et al., 2016; Kamaleson et al., 2019) but this does not occur off northern part of Indian west coast as a strong pycnocline prevents the entrainment of subsurface water to surface (Naqvi et al., 2006). This is also evident from the contrasting vertical profiles of temperature and salinity between C1 (Calicut), and B2 (off Mumbai), (G3-G6) off Goa, K3 (off Karwar) and (M1, M3) off Mangalore (Fig. 4-6). At the latter four transects, there is a warm ($>26^\circ\text{C}$), low saline (<34) water layer at the surface whereas at C1, the surface layer is cooler ($<26^\circ\text{C}$) and more saline (~ 35). Thus, the upwelled water apparently surfaced at C1, which was not the case at the other northern stations, which caused some portion of S^0 surfaced as plumes near off Calicut whereas it got oxidized to SO_4^{2-} within the subsurface anoxic depths at Mangalore, Karwar, Goa and Mumbai. However, it only indicated that at C1, the rate of S^0 accumulation (at surface) exceeded its oxidation to SO_4^{2-} , and did not rule out the oxidation of the rest of S^0 to SO_4^{2-} in the subsurface waters.

To further investigate the response of denitrification to sulfide, we tested denitrification rates as a function of sulfide concentration (Suppl. fig. 11) wherein we observed a strong positive correlation ($r^2 > 0.9$) between denitrification rate and sulfide concentration at 5 depths, with the rates attaining maxima at $10\ \mu\text{M}\ \text{S}^{2-}$. But at most of the depths, we observed the denitrification rates either reaching maxima at $5\ \mu\text{M}\ \text{S}^{2-}$ or increasing non-linearly or decreasing beyond that as also observed elsewhere (Hietanen et al., 2012). Similar sulphide dependency of denitrification has been reported in other anoxic coastal systems as well (Jensen et al., 2009; Dalsgaard et al., 2013; Galan et al., 2014; Michiels et al., 2019). These results indicate that the denitrification in the WICS waters is stimulated by sulphide up to 5-10 μM beyond which it is either saturated or inhibited. The response of denitrification to increasing sulphide levels can vary among various systems due to specific adaptive capability of a particular group of denitrifiers to a specific physico-biogeochemical condition of the system (Bonaglia et al., 2016). For instance, Dalsgaard et al. (2013) and Jensen et al. (2009) did not observe any saturation or inhibition in

denitrification up to 10 μM and 40 μM sulphide, respectively, whereas Bonaglia et al. (2016) reported a saturation or inhibition in denitrification at ≥ 2 μM sulphide which was due to the inhibition of the reductase enzyme catalyzing the last step of denitrification.

During September-October, colorless sulphur-oxidizing bacteria (Kamaleson et al., 2019) and particularly, *Thiobacillus denitrificans* like organism (Krishnan et al., 2008), a sulphur-oxidizing denitrifier belonging to β -proteobacteria prevail in the suboxic/anoxic subsurface waters of the WICS. More recent studies have detected a culturable sulphur-oxidizing denitrifiers such as *Marinobacter hydrocarbonoclasticus* (Gomes et al., 2020) and other sulfur-oxidizing denitrifiers belonging to clade SUP05, and groups *Thiomicrothrix sp.*, *Marinobacterium sp.*, *Alcanivorax sp.* and *Vibrio sp.* in the suboxic/anoxic WICS waters through V3-V4 sequencing of the 16S rRNA (Naik et al., *under review*). Hence, our combined results from in-situ rate experiments, bag incubations, sulfur plume imaging and detection of sulfur-oxidizing chemoautotrophic denitrifiers strongly indicated that that the denitrification over the WICS was largely driven and/or stimulated by sulphide, being carried out by sulphur-oxidizing chemolithotrophs in the anoxic WICS waters.

4.4. Relative contribution of chemoorganotrophic and chemolithotrophic (sulfide-driven) denitrification

Although we have strong evidence that sulphide driven denitrification was occurring, we cannot exclude that there was co-occurring non-sulphide driven denitrification i.e. chemoorganotrophic denitrification coupled to organic matter oxidation. Previous studies based on PCR amplification of *nirS* and *nirK* genes, and DNA sequencing have revealed the presence of a diverse, presumably chemoorganotrophic denitrifiers dominating the suboxic shelf waters during the early phase of denitrification (July-August) (Jayakumar et al., 2004; Gomes et al., 2018). The occurrence of chemoorganotrophic denitrification in August has also been observed based on its biogeochemical signatures in the bag (Naqvi et al., 2000) and ^{15}N -labelled incubations (Sarkar et al., 2020) of the NO_x^- -rich suboxic (sulphide free) shelf waters. Therefore, based on the prevailing biogeochemical conditions at stations B2, G6, K3 and M3, where the water column was suboxic (i.e. sulphide-free and NO_x^- -replete), all of the denitrification in the experiments with only $^{15}\text{NO}_2^-$ addition appears to be chemoorganotrophic with a the mean rate of $342 (\pm 296)$ $\text{nmol N}_2 \text{ L}^{-1} \text{ d}^{-1}$ at these stations. In a very similar case, Dalsgaard et al. (2013) and Bonaglia et al. (2016) experimentally showed the occurrence of chemoorganotrophic denitrification within the NO_x^- -replete, sulphide free chemocline of the Baltic Sea. However, the stimulation in denitrification rates by 1.7-14 folds at these suboxic stations upon $^{15}\text{NO}_2^- + \text{S}^{2-}$ addition indicated (1) the presence of sulfide-oxidizing denitrifiers in these suboxic waters and (2) the potential occurrence of sulfide-driven denitrification up to rates of $1613 (\pm 1070)$ nmol

$\text{N}_2 \text{ L}^{-1} \text{ d}^{-1}$. Since our sampling period was only up to 1st week of October, we did not observe sulphidic conditions at these stations, however they are known to turn sulphidic during late SW monsoon (Naqvi et al., 2000, 2006, 2009; Shirodkar et al., 2018; Sarkar et al., 2020), whereupon we speculate that the denitrification rate would increase.

Although, H_2S in the WICS waters is known to vary spatially and annually, the average of maximum H_2S concentration reported from a decade long observation (Naqvi et al., 2009) can be considered as $\sim 5 \mu\text{M}$ which is close to the maximum H_2S observed in our study i.e. $6 \mu\text{M}$. Therefore, the denitrification rates observed with $^{15}\text{NO}_2^- + 5 \mu\text{M S}^{2-}$ addition can closely represent the actual/potential sulfide-driven denitrification rates in the shelf waters. Precisely, at the sulphidic stations (i.e. G3, G4, G5, M1 and C1), the rates (mean: $3347 \pm 1298 \text{ nmol N}_2 \text{ L}^{-1} \text{ d}^{-1}$) can be considered as the actual denitrification rates whereas at the suboxic stations (i.e. B2, G6, K3 and M3), the rates (mean: $1614 \pm 1070 \text{ nmol N}_2 \text{ L}^{-1} \text{ d}^{-1}$) can be considered as the potential denitrification rates. Considering the rates at all the stations and depths, the mean rate of sulfide-driven denitrification was observed to be $2697 (\pm 1464) \text{ nmol N}_2 \text{ L}^{-1} \text{ d}^{-1}$ in the shelf waters whereas anammox and DNRA occurred at mean rates of $16.5 \text{ nmol N}_2 \text{ L}^{-1} \text{ d}^{-1}$ and $48.7 \text{ nmol N L}^{-1} \text{ d}^{-1}$, respectively. This showed that our mean actual sulfide-driven denitrification rate (i.e. $3.34 \mu\text{M N}_2 \text{ d}^{-1}$) was very similar to the denitrification rate (i.e. $3.21 \mu\text{M N}_2 \text{ d}^{-1}$) reported by Sarkar et al. (2020) during the sulphidic event of 2009. A comparative analysis of the sulfide driven denitrification rates, anammox and DNRA rates among the anoxic coastal systems of the world (Table 4) shows that the highest sulfide-driven denitrification rate we observed over the WICS ($11650 \text{ nmol N L}^{-1} \text{ d}^{-1}$, off Calicut) is one of the highest in the world, being second only to the rate observed in the Mariager Fjord ($37200 \text{ nmol N L}^{-1} \text{ d}^{-1}$; Jensen et al., 2009). Considering our mean rate of chemoorganotrophic denitrification as $342 (\pm 296) \text{ nmol N}_2 \text{ L}^{-1} \text{ d}^{-1}$ observed at the suboxic stations and the denitrification rate reported by Sarkar et al. (2020) during suboxic years (i.e. $1.53 \mu\text{M N}_2 \text{ d}^{-1}$), it appears that with the advent of sulphidic event, sulfide-driven denitrification replaces chemoorganotrophic denitrification as the dominant N loss process and causes massive N loss at a rate 2-8 times faster than that via chemoorganotrophic denitrification over the WICS.

Coastal system, Location	Maximum H ₂ S (μM)	Autotrophic denitrification (nM N d ⁻¹)	Anammox (nM N d ⁻¹)	DNRA (nM N d ⁻¹)	Reference
Golfo Dulce Bay, Costa Rica	1.8	48-5184	72-450	n.m.	Dalsgaard et al. (2003)
Baltic Sea	110	100-5400	10-100	20-510	Hannig et al. (2007)
	62	440-9318	10-18	n.m.	Hietanen et al. (2012)
	40	11-763	n.d.	n.m.	Dalsgaard et al. (2013)
	175	490-3813	1.7-7.4	100-432	Bonaglia et al. (2016)
	277	100-37200	n.d.	n.m.	Jensen et al. (2009)
Mariager Fjord, Denmark	277	100-37200	n.d.	n.m.	Jensen et al. (2009)
Namibian Shelf	18	n.d.-560	n.d.-140	n.m.	Lavik et al. (2009)
Peruvian Shelf	4.2	33-490	50-250	4-40	Schunk et al. (2013)
Chilean Shelf	~15	n.d.-2322	n.d.-206	n.m.	Galán et al. (2014)
Saanich Inlet, Canada	41	13-6720	40-633	n.m.	Michiels et al. (2019)
Western Indian Shelf	6	920-11650	n.d.-238	16-182	This study

Table 4. A comparison of the rates of autotrophic denitrification, and anammox and DNRA observed in various anoxic coastal systems of the world. n.d.: not detected, n.m.: not measured.

4.5. Optimum, limitation and sustenance of autotrophic denitrification:

During September, the prevailing shelf biogeochemistry primes the conditions for the occurrence sulfide driven denitrification as the suboxic water column still carries a modest amount of NO_x⁻ (mainly NO₂⁻), and receives significant sulphide flux from the sediments (i.e. 4.3 mmol m⁻² d⁻¹; Pratihary et al., 2014). The vertical velocity of upwelling over the WICS i.e. 2.77×10⁻² cm s⁻¹ (Unnikrishnan and Antony, 1990), suggests that the benthic-released sulphide would result in sulphide accumulation at the rate of 0.39 μmol L⁻¹ d⁻¹ in the 11 m-thick SMZ. The pelagic sulphide generation rate i.e. 1.17 μmol L⁻¹ d⁻¹ (Pratihary et al., *manuscript in preparation*) would further increase the total sulphide accumulation rate to 1.56 μmol L⁻¹ d⁻¹. But the sulphide oxidation rate measured from the bag incubation i.e. 3.84 μmol L⁻¹ d⁻¹ (Section 3.4) or estimated from the mean sulfide-driven denitrification rate (2.69 μM N₂ d⁻¹) using HS⁻:N₂ ratio (Eq. 1) i.e. 3.37 μmol L⁻¹ d⁻¹ was >2 fold higher than the sulphide accumulation rate. Consistently, Kamaleson et al. (2019) have reported much higher rates of sulfur-oxidizing activity (SOA) than sulfate-reducing activity (SRA) in the near-suboxic (sulphidic-free) shelf waters of Southwest India. This suggested that the chemolithoautotrophic denitrifiers have the potential to oxidize 100% of the sulphide accumulated in the water column or at least at the suboxic-anoxic interface as long as they are not limited by NO_x⁻ availability, which is evident from the fact that during early September, we often observe the shelf bottom water to be NO_x⁻-depleted but not sulphidic yet (Naqvi et al., 2006). This indicates a cryptic occurrence of sulfide driven denitrification in the shelf bottom water precisely due to rapid oxidation of benthic-released sulphide by NO₂⁻ of the overlying suboxic water creating an impression of NO₂⁻-depleted, non-sulphidic condition in the bottom water. A similar observation over the Namibian Shelf led Lavik et al. (2009) to postulate that many anoxic events in the coastal waters are probably not noticed due

to faster and efficient oxidation of sulphide by NO_x^- , mediated by proliferating chemolithoautotrophs. This further suggested a possible co-occurrence heterotrophic denitrification in the NO_x^- -rich suboxic intermediate layer and autotrophic denitrification in the underlying anoxic bottom water (Fig. 9a). Consequently, it would create an optimal condition for the autotrophic denitrification causing massive N loss over the WICS due to adequacy of substrates as NO_2^- is supplied through heterotrophic denitrification in the overlying water and sulphide is supplied through SO_4^{2-} reduction in the underlying sediments. As the NO_x^- inventory is efficiently depleted through autotrophic denitrification at the suboxic-anoxic interface, the thickness of suboxic layer wanes away progressively, and the sulphidic layer expands upward.

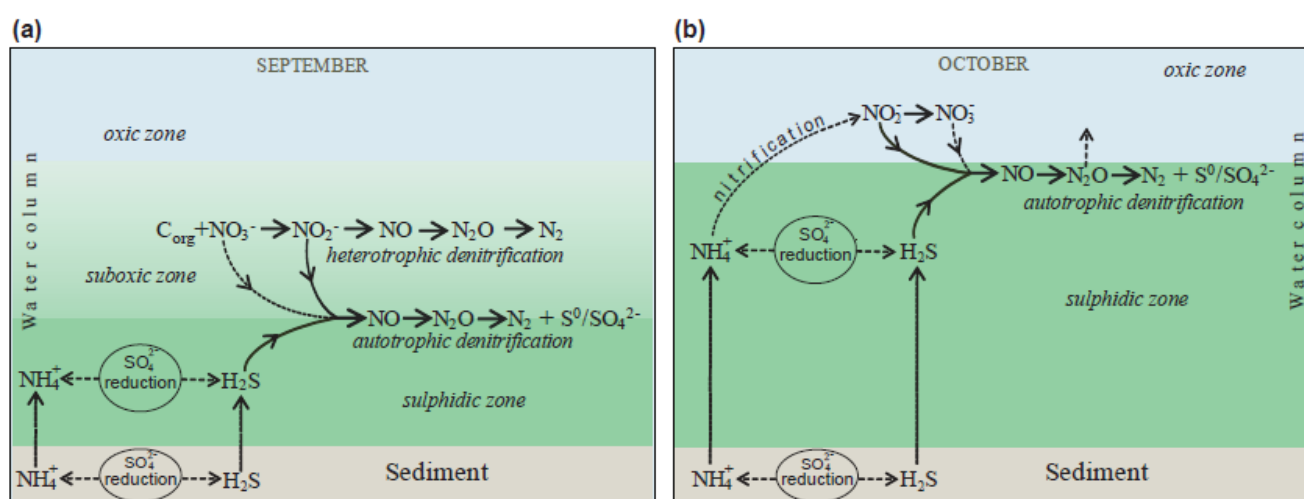


Fig.9. A conceptual overview of the denitrification pathways in the WICS waters during (a) September and (b) October.

However, by early October, as the NO_x^- -replete suboxic layer disappears completely and is replaced by NH_4^+ -rich but NO_x^- -depleted sulphidic layer; it leads to two layer stratification (i.e. oxic and anoxic) of the shelf water column (Naqvi et al., 2006). Although, the autotrophic denitrification is expected to be limited by NO_x^- during this period, our measured high potential rate of autotrophic denitrification in the sulphidic bottom water indicated the abundance and growth of chemolithoautotrophs which are possibly sustained by NO_x^- supply through nitrification. Having a high diffusive coefficient (Schulz, 2006), NH_4^+ in the sulphidic bottom water will be transported upwards by diffusion and turbulent mixing (Holtermann and Umlauf, 2012) and gets nitrified to NO_x^- at the oxic-anoxic interface, which in turn is transported below the interface by the same processes to potentially support sulphide driven denitrification (Fig. 9b). Such a coupling of nitrification and denitrification leading to higher N loss has been experimentally observed in the WICS waters (Krishnan et al., 2008) and elsewhere (Hietanen et al., 2012; Kalvelage et al., 2015). Although, the abundance of nitrifying bacteria in the anoxic shelf waters remains below

detection (Krishnan et al., 2008), the possible proliferation of ammonium oxidizing archaea (AOA) cannot be ruled out. Unlike ammonium oxidizing bacteria (AOB) which cannot survive in sulphidic condition (Joye and Hollibaugh, 1995), AOA can thrive in sulphidic waters (Ergruder et al., 2009) with sulphide reaching up to 30 μM (Coolen et al., 2007). Thus, the sulfide driven denitrification is possibly fed by archaeal nitrification in the NO_x^- -depleted sulphidic shelf water as also observed by Hietanen et al. (2012) and Berg et al. (2015) in the Baltic Sea. Therefore, during October, the sulfide-driven denitrification is possibly sustained by being coupled to nitrification, and continues to cause N loss even in under NO_x^- -limiting conditions.

4.6. Impact of sulphide on N_2O cycling:

During our study, at the sulphidic stations, we frequently observed prominent N_2O peaks just at or above the oxic-anoxic interface, but very low N_2O in the sulphidic bottom water. A similar pattern of N_2O distribution is frequently observed during suboxia-anoxia transition phase over the WICS (Naqvi et al., 2006) and also in other sulphidic coastal systems (Brettar and Rheinheimer, 1991; Schunk et al., 2013). Such high and disproportionate N_2O build-up at the oxic-anoxic interface is therefore likely to be occurring due to (1) partial inhibition of N_2O reduction under microaerobic conditions (Naqvi et al., 2000; Dalsgaard et al., 2014; Arévalo-Martínez et al., 2015), (2) suppressed N_2O reductase enzyme (nosZ) activity is due to limitation of Cu (Granger and Ward, 2003; Sullivan et al., 2013) which precipitates with sulphide (Callbeck et al., 2021), and/or (3) N_2O production as a byproduct of ammonia oxidation occurring at low O_2 concentrations (Löscher et al., 2012; Xi et al., 2015). Our ^{15}N incubations showed much higher transient N_2O production with $^{15}\text{NO}_2^- + \text{S}^{2-}$ compared to $^{15}\text{NO}_2^-$ (Suppl. fig. 3-10) at all the stations irrespective of them being suboxic or anoxic. After sulphide addition, concomitant with the higher N_2 production, transient N_2O accumulation increased by 1.4-44 fold at the suboxic stations and by 1.2-18 fold at the anoxic stations (Suppl. fig. 12). As the oxic-anoxic interface of the WICS water column is possibly subjected to frequent aeration (Naqvi et al., 2006) the further reduction of such high amounts of N_2O (to N_2) could be inhibited in situ, explaining its build-up at or just above the oxic-anoxic interface.

Contrastingly, non-detectable to undersaturated N_2O concentrations observed in the sulphidic bottom waters (Fig. 5, 6) was apparently due to its effective reduction to N_2 as evidenced in our $^{15}\text{NO}_2^- + \text{S}^{2-}$ -amended incubations and bag incubations. Although, transient N_2O production was higher in the $^{15}\text{NO}_2^- + \text{S}^{2-}$ incubations than in the $^{15}\text{NO}_2^-$ incubations (Suppl. fig. 3-10, 12), there was no clear trend in the ratio of N_2 to N_2O production, and net N_2O consumption also began earlier in the $^{15}\text{NO}_2^- + \text{S}^{2-}$ incubations than in the $^{15}\text{NO}_2^-$ incubations. This indicated that N_2O produced through sulphide-driven denitrification is more effectively reduced to N_2 than during chemoorganotrophic denitrification, supporting evidence that

sulfide oxidizing denitrifiers have a high level of tolerance to sulphide (Jensen et al., 2009) and indicating that the sulfide-driven denitrifiers in the WICS are capable of complete denitrification of NO_x^- to N_2 as reported in the Baltic Sea (Heitenan et al., 2012) and ETSP (Callbeck et al., 2018).

4.7. Chemoautotrophy and dark CO_2 fixation:

Chemolithoautotrophic denitrifiers are known to fix CO_2 via reductive/reverse tricarboxylic acid (rTCA) cycle by using the energy gained from sulphide oxidation by NO_x^- (Campbell et al., 2006; Shao et al., 2010). Cultivated chemoautotrophic sulphide oxidizers have been observed to fix 0.22-0.37 mole of CO_2 per mole of NO_x^- reduced or 0.62 mole of H_2S oxidized (Callbeck et al., 2018 and references therein). Considering the mean autotrophic denitrification rate ($2.69 \mu\text{mol N}_2 \text{ L}^{-1} \text{ d}^{-1}$) and the $\text{N}_2:\text{NO}_x^-$ ratio (Eq. 1), the mean NO_2^- consumption rate would be $0.22 \mu\text{mol L}^{-1} \text{ h}^{-1}$ in the ^{15}N incubations, which is similar to the NO_2^- consumption rate observed in bag incubations i.e. $0.27 (\pm 0.07) \mu\text{mol L}^{-1} \text{ h}^{-1}$ (Section 3.4, Fig. 8). Considering the former rate, chemoautotrophically fixed CO_2 was conservatively estimated to be $1.18\text{-}1.98 \mu\text{mol C L}^{-1} \text{ d}^{-1}$ which amounts to a mean depth-integrated rate of $0.21 (\pm 0.07) \text{ g C m}^{-2} \text{ d}^{-1}$ assuming an 11 m-thick SMZ. The average primary productivity over the shelf during seasonal anoxia (September-October) i.e. $1.15 (\pm 0.7) \text{ g C m}^{-2} \text{ d}^{-1}$ (Gauns et al., 2020) suggests that the chemoautotrophic (dark) C production was 18% of the photoautotrophic production and accounted for 15% of the total water column productivity. Jørgensen et al. (1991) observed dark CO_2 fixation rate occurring at the rate of $24\text{-}63 \text{ mg C m}^{-2} \text{ d}^{-1}$ and comprising 4-11% of the total primary production in the Black Sea. Tayler et al. (2001) reported that dark C fixation occurred at a rate of $0.32\text{-}1.9 \text{ g C m}^{-2} \text{ d}^{-1}$ which was 62% of the photoautotrophic C production in the Cariaco basin. Schunck et al. (2013) reported that dark C fixation with a rate of $10.8\text{-}16.8 \mu\text{g C L}^{-1} \text{ d}^{-1}$ accounted for 25% of the total CO_2 fixation over the Peruvian shelf. Thus, the dark CO_2 fixation rate and its contribution to total autotrophic C productivity over the WICS are comparable to those reported in the other anoxic coastal systems (Jørgensen et al., 1991; Tayler et al., 2001; Schunck et al., 2013) of the world.

4.8. Impact of chemolithoautotrophic denitrification on N, S and C budget of the WICS

Over the WICS, sulphidic condition develops in the bottom water during early/mid September while the water column still has some amount of NO_x^- . By early October, the sulphidic condition spreads to a greater area of the shelf but the water column remains NO_x^- -depleted. During late SW monsoon, $60,000 \text{ Km}^2$ areas of the WICS is considered to be functionally anoxic or denitrifying (Sarkar et al., 2020) which covers the innershelf and mid-shelf. However, by conservative estimates, the sulphidic zone occupies an area of $16,000 \text{ Km}^2$ of the innershelf, and the occurrence of sulphidic bottom water underlain by or interspersed with NO_x^- -rich suboxic water persists at least for 1 month. Thus, considering the above

factors, and 11 m as the average thickness and $17.6 \times 10^{10} \text{ m}^3$ as the volume of the SMZ, and mean N loss/transformation rates (Section 4.4), the N loss rate due to autotrophic denitrification and anammox were 0.4 Tg N y^{-1} and $0.002 \text{ Tg N y}^{-1}$, respectively whereas N transformation rate due to DNRA was $0.004 \text{ Tg N y}^{-1}$. Previously, using NO_3^- consumption rate and assuming heterotrophic denitrification as the dominant N loss process, Naqvi et al. (2006) had estimated the N loss to be 1.3 Tg N y^{-1} . However, using ^{15}N incubations and considering the mean denitrification rate from a sulphidic year and two non-sulphidic (suboxic) years, Sarkar et al. (2020) reported the N loss rate to be 3.7 Tg N y^{-1} . The difference between the estimated annual N loss rates reported by the above authors and us arises apparently due to their consideration of denitrification occurring over a larger area ($60,000 \text{ Km}^2$), broader depth range (20 m) and longer duration i.e. 90 days (August-October). Thus, considering the conservative estimate by Sarkar et al. (2020), the autotrophic denitrification would account for $\sim 11\%$ of the total annual N loss in the shelf waters during seasonal anoxia. Additionally, chemolithoautotrophic denitrifiers potentially remove or oxidize 0.57 Tg of toxic sulphide from the shelf waters annually, taking the mean autotrophic denitrification rate and $\text{HS}^-:\text{N}_2$ ratio (Eq. 1) into account. This is probably the reason for the much lower sulphide accumulation in the anoxic WICS water compared to other anoxic shallow marine systems of the world (Table 4). Upscaling of the estimated dark C fixation rate i.e. $0.21 \text{ g C m}^{-2} \text{ d}^{-1}$ over the anoxic shelf leads to an annual chemoautotrophic C fixation at the rate of 0.1 Tg C y^{-1} . Therefore, the prevalence of chemolithoautotrophic denitrification in the shelf waters can potentially impact the pelagic N, S and C budget of the WICS by removing significant quantity of extraneous N, toxic sulphide, and by adding extra C_{org} .

4.9. Implications for shelf biogeochemistry

Sulphide is toxic or lethal for many marine organisms (Petersen, 1977; Nicholls and Kim, 1982; Levin et al., 2009; Vaquer-Sunyer and Duarte 2010) and as such, the abundance of many demersal fishes and benthic organisms are substantially reduced during sulphidic events on the WICS (Naqvi et al., 2006; Naqvi et al. 2009; Ingole et al., 2010). Our study implies that sulphide-driven autotrophic denitrification plays a crucial role in minimizing sulphide toxicity in the shelf waters. Although, sulphide is detected in the shelf bottom water around mid-September, NO_x^- is depleted in the same waters around a month earlier. It is highly likely that during this time the cryptic occurrence of sulphide-driven denitrification (supplied with NO_x^- diffusing from oxycline, see Fig 9), is responsible for the removal of H_2S and thereby it detoxifies the shelf bottom water during mid August to early September. Even from mid to late September, sulphide levels remain low which is apparently due to its effective oxidation via autotrophic denitrification. Consequently, for about a month (mid August to mid September), the shelf bottom water is effectively detoxified. Chemolithoautotrophic denitrification also seems to provide other crucial

ecosystem services on the western Indian shelf as the sulphidic waters appear to be an effective sink for N₂O, partially ameliorating the massive accumulations of this potent greenhouse gas that occur at oxycline. Efficient carbon retention through dark CO₂ fixation possibly sustains the intensity and the duration of euxinic regime over the shelf. Thus, by causing rapid NO_x⁻ loss, sulphide oxidation and significant dark CO₂ fixation, chemolithoautotrophic denitrification reduces N₂O and CO₂ emission, retains carbon in the shelf system and links three key elements *i.e.* C, N and S of the shelf biogeochemical cycle. With the increasing expansion and intensification of OMZs, increase in the number of dead zones and increasing frequency in sulphidic events, chemolithoautotrophic denitrification is expected to play a greater role in N cycling and budget of shallow marine systems in future.

Acknowledgements

The authors wish to thank the Director, CSIR-National Institute of Oceanography (NIO) for providing logistics and laboratory facility for this work which was carried out as AP's post-doctoral research that formed a part of collaborative programme between NIO and MPIMM. AP gratefully acknowledges DAAD (German Academic Exchange Service) for the Post-doctoral Fellowship and funding this research programme. SWAN acknowledges the European Commission for the Marie Curie International Incoming Fellowship. AS and GS duly acknowledge CSIR for the Senior Research Fellowships. HKM was funded by the DFG Cluster of Excellence "The Ocean Floor – Earth's Uncharted Interface" at MARUM, University of Bremen (EXC-2077). We also thank Gabi Klockgether, Goudong Song and Jessika Füssel for their kind help in the analyses at MPIMM. Ankita Chari and Sushma Naik are duly acknowledged for their assistance in nutrients and N₂O analysis, respectively. The MERIS data were kindly provided by ESA. We thankfully acknowledge the use of MODIS data from LANCE FIRMS operated by the NASA/GSFC/Earth Science Data and Information System (ESDIS) with funding provided by NASA/HQ. We thank Dr. I. Suresh for the valuable discussion. The captain and crew of *R/V Sindhu Sankalp* (SSK-24) are duly acknowledged for their kind help and logistic support. This research work was also partly funded by CSIR through NIO's network project PSC0108, and by MoES through the SIBER-India project GAP2425. This is CSIR-NIO's contribution no. xxxx.

References

- Aelion, C. M., Warttinger, U., 2010. Sulfide inhibition of nitrate removal in coastal sediments. *Estuar. Coast.* 33, 798–803.
- Arévalo-Martínez, D.L., Kock, A., Löscher, C.R., Schmitz, R.A., Bange, H.W., 2015. Massive nitrous oxide emissions from the tropical South Pacific Ocean. *Nat. Geosci.* 8, 530-535.
- Bardhan P., Naqvi, S. W. A., 2020. Nitrogen and carbon cycling over the western continental shelf of India during seasonal anoxia: A stable isotope approach. *J. Mar. Syst.* 207, 103144.

- Berg, C., Vandieken, V., Thamdrup, B., Jürgens, K., 2015. Significance of archaeal nitrification in hypoxic waters of the Baltic Sea. *The ISME J.* 9, 1319-1332.
- Bernard, R. J., Mortazavi, B., Kleinhuizan, A. A., 2015. Dissimilatory nitrate reduction to ammonium (DNRA) seasonally dominates NO_3^- reduction pathways in an anthropogenically impacted sub-tropical coastal lagoon. *Biogeochemistry* 125, 47-64.
- Bonaglia, S., Klawonn, I., Brabandere, L. D., Deutsch, B., Thamdrup, B., Brüchert, V., 2016. Denitrification and DNRA at the Baltic Sea oxic-anoxic interface: Substrate spectrum and kinetics. *Limnol. Oceanogr.* 61, 1900-1915.
- Breitburg, D., Levin, L.A., Oschlies, A., Grégoire, M., Chavez, F.P., Conley, D.J., Garçon, V., Gilbert, D., Gutierrez, D., Isensee, K., Jacinto, G.S., Limberg, K.E., Montes, I., Naqvi, S.W.A., Pitcher, G.C., Rabalais, N.N., Roman, M.R., Rose, K.A., Seibel, B.A., Telszewski, M., Yasuhara, M., Zhang, J., 2018. Declining oxygen in the global ocean and coastal waters. *Science* 359, eaam7240, DOI:10.1126/science.aam7240.
- Brettar, I., Rheinheimer, G., 1991. Denitrification in the Central Baltic Sea: evidence for H_2S -oxidation as motor of denitrification at the oxic-anoxic interface. *Mar. Ecol. Prog. Ser.* 77, 157-169.
- Brettar, I., Labrenz, M., Flavier, S., Bötel, J., Kuosa, H., Christen, R., Höfle, M.G., 2006. Identification of a *Thiomicrospira denitrificans*-Like Epsilonproteobacterium as a catalyst for autotrophic denitrification in the Central Baltic Sea. *Appl. Environ. Microbiol.* 72 (2), 1364-1372.
- Bristow, L.A., Dalsgaard, T., Tiano, L., Mills, D.B., Bertagnolli, A.D., Wright, J.J., Hallam, S.J., Ulloa, O., Canfield, D.E., Revsbech, N.P., Thamdrup, B., 2016. Ammonium and nitrite oxidation at nanomolar oxygen concentrations in oxygen minimum zone waters. *PNAS* 113 (38), 10601-10606.
- Brunet, R.C., Garcia-Gil, L.J., 1996. Sulfide-induced dissimilatory nitrate reduction to ammonia in anaerobic freshwater sediments. *FEMS Microbiol. Ecol.* 21, 131-138.
- Burgin, A.J., Hamilton, S.K., 2008. NO_3^- -driven SO_4^{2-} production in freshwater ecosystems: Implications for N and S cycling. *Ecosystems* 11, 908-922.
- Campbell, B.J., Engel, A.S., Porter M.L., Takai, K., 2006. The versatile ϵ -proteobacteria: key players in sulphidic habitats. *Nature Reviews Microbiology* 4, 458-468.
- Callbeck, C. M., Lavik, G., Ferdelman, T.G., Fuchs, B., Gruber-Vodicka, H.R., Hach, P.F., Littman, S., Schoffelen, N.J., Kalvelage, T., Thomsen, S., Schunck, H., Loscher, C.R., Schmitz, R.A., 2018. Oxygen minimum zone cryptic sulphur cycling sustained by offshore transport of key sulphur oxidizing bacteria. *Nat. Commun.* 9, 1-11.
- Callbeck, C.M., Pelzer, C., Lavik, G., Ferdelman, T.G., Graf, J.S., Vekeman, B., Schunck, H., Littman, S., Fuchs, B.M., Hach, P.H., Kalvelage, T., Schmitz, R.A., Kuypers, M.M.M., 2019. *Archobacter peruensis* sp. nov., a chemolithoheterotrophs isolated from sulfide- and organic-rich coastal waters off Peru. *Appl. Environ. Microbiol.* 58 (24), e01344-19.
- Canfield D. E., Stewart, F. J., Thamdrup, B., De Brabandere, L., Dalsgaard, T., Delong, E. F., Revsbech, N. P., Ulloa, O., 2010. A cryptic sulphur cycle in the oxygen-minimum-zone waters off the Chilean coast. *Science* 330, 1375-1378.
- Castro-González, M., Fariás L., 2004. N_2O cycling at the core of the oxygen minimum zone off northern Chile. *Mar. Ecol. Prog. Ser.* 280, 1-11.

- Cline, J. D. 1969. Spectrophotometric determination of hydrogen sulphide in natural waters. *Limnol. Oceanogr.* 14: 454-458.
- Codispoti, L. A., 1989. Phosphorus vs. nitrogen limitation of new and export production, p. 377-394. In W. H. Berger, V. S. Smetacek and G. Wefer [eds.], *Productivity of the Ocean: Present and Past*. John Wiley.
- Codispoti, L. A., Brandes, J. A., Christensen, J. P., Devol, A. H., Naqvi, S. W. A., Paerl, H. W., Yoshinari, T., 2001. The oceanic fixed nitrogen and nitrous oxide budgets: Moving targets as we enter the anthropocene? *Sci. Mar.* 65, 85-105.
- Coolen, M.J.L., Abbas, B., Van Bleijswijk, J., Hopmans E.C., Kuypers, M.M.M., Wakeham S.G., 2007. Putative ammonia-oxidizing Crenarchaeota in suboxic waters of the Black Sea: a basin-wide ecological study using 16S ribosomal and functional genes and membrane lipids. *Environ. Microbiol.* 9, 1001-1016.
- Dalsgaard, T., Canfield, D. E., Petersen, J., Thamdrup, B., Acuña-González, J., 2003. N₂ production by the anammox reaction in the anoxic water column of Golfo Dulce, Costa Rica. *Nature* 422, 606-608.
- Dalsgaard, T., Brabandere, L. D., Hall, P. O. J., 2013. Denitrification in the water column of the central Baltic Sea. *Geochim. Cosmochim. Acta* 106, 247-260.
- Dalsgaard, T., Stewart, F.J., Thamdrup, B., De Brabandere, L., Revsbech, N.P., Ulloa, O., Canfield, D.E., DeLong, E.F., 2014. Oxygen at nanomolar levels reversibly suppresses process rates and gene expression in anammox and denitrification in the oxygen minimum zone off Northern Chile. *Am. Soc. Microbiol.* 5 (6), e01966-14.
- De Brabandere, L., Canfield, D.E., Dalsgaard, T., Friederich, G.E., Revsbech, N.P., Ulloa, O., Thamdrup, B., 2014. Vertical partitioning of nitrogen-loss processes across the oxic-anoxic interface of an oceanic oxygen minimum zone. *Environ. Microbiol.* 16 (10), 3041-3054.
- Diaz, R. J., Rosenberg, R., 2008. Spreading dead zones and consequences for marine ecosystems. *Science* 321, 926-929.
- Ergruder, T.H., Boon, N., Wittebolle, L., Marzorati, M., Verstraete, W., 2009. Environmental factors shaping the ecological niches of ammonia-oxidizing archaea. *FEMS Microbiol. Rev.* 33, 855-869.
- Falkowski, P.G., Evolution of the nitrogen cycle and its influence on the biological sequestration of CO₂ in the ocean. *Nature* 387, 272-275.
- Fuchsman, C. A., Murray, J. W., Staley, J. T., 2012. Stimulation of autotrophic denitrification by intrusions of the Bosphorus Plume into the anoxic Black Sea. *Front. Microbiol.* 3, 1- 14.
- Füssel, J., Lam, P., Lavik, G., Jensen, M.M., Holtappels, M., Günter, M., Kuypers, M.M.M., 2012. Nitrite oxidation in the Namibian oxygen minimum zone. *The ISME J.* 6, 1200-1209
- Galán, A., Faúndez, J., Thamdrup, B., Santibáñez, J. F., Farías, L., 2014. Temporal dynamics of nitrogen loss in the coastal upwelling ecosystem off central Chile: Evidence of autotrophic denitrification through sulfide oxidation. *Limnol. Oceanogr.* 59(6), 1865-1878.
- Gauns, M., Mochemadkar, S., Pratihary, A., Shirodkar, G., Narvekar, P.V., Naqvi, S.W.A., 2020. Phytoplankton associated with seasonal oxygen depletion in waters of the western continental shelf of India. *J. Mar. Syst.* 204, 103308.
- Gilbert, D., Rabalais, N.N., Díaz, R.J., Zhang, J., 2010. Evidence for greater oxygen decline rates in the coastal ocean than in the open ocean. *Biogeosciences* 7, 2283-2296.

- Glaubitz, S., Leuders, T., Abraham, W.R., Jost, G., Jürgens, K., Labrenz, M., 2009. ^{13}C -isotope analyses reveal that chemolithoautotrophic Gamma- and Epsilonproteobacteria feed microbial food web in a pelagic redoxclines of the Central Baltic Sea. *Environ. Microbiol.* 11(2), 326-337.
- Glaubitz, S., Labrenz, M., Jost G., Jürgens, K., 2010. Diversity of active chemolithoautotrophic prokaryotes in the sulfidic zone of a Black Sea pelagic redoxclines as determined by rRNA-based stable isotope probing. *FEMS Microbiol. Ecol.* 74, 32-41.
- Glaubitz, S., Kießlich, K., Meeske, C., Labrenz, M., Jürgens, K., 2013. SUP05 dominates the Gammaproteobacterial sulfur oxidizer assemblages in pelagic redoxclines of the Central Baltic and Black Sea. *Appl. Environ. Microbiol.* 79 (8), 2767-2776.
- Gomes, J., Khandeparker, R., Bandekar, M., Meena, R.M., Ramaiah, N., 2018. Quantitative analyses of denitrifying bacterial diversity from a seasonally hypoxic monsoon governed tropical coastal region. *Deep Sea Res. II* 34-43.
- Gomes J., Khandeparker, R., Meena, R.M., Ramaiah, N., 2019. Bacterial community composition markedly altered by coastal hypoxia. *Ind. J. Microbiol.* 59 (2), 200-208.
- Gomes J., Khandeparker, R., Naik, H., Shenoy, D., Meena R.M., Ramaiah, N., 2020. Denitrification rates of culturable bacteria from a coastal location turning temporally hypoxic. *J. Mar. Syst.* 209, 103089.
- Granger, J., Ward, B.B., 2003. Accumulation of nitrogen oxides in copper-limited cultures of denitrifying bacteria. *Limnol. Oceanogr.*, 48(1), 2003, 313-318.
- Grasshoff, K., Kremling, K., Ehrhardt, M., 1999. *Methods of Seawater Analysis*, 3rd ed. Wiley-VCH Verlag GmbH.
- Grote, J., Schott, T., Bruckner, C. G., Glöckner, F. O., Jost, G., Teeling, H., Labrenz, M., Jürgens, K., 2012. Genome and physiology of a model Epsilonproteobacterium responsible for sulfide detoxification in marine oxygen depletion zones. *Proc. Natl. Acad. Sci.* 109, 506-510.
- Gruber N., Sarmiento, J. L., 2002. Large-scale biogeochemical-physical interactions in elemental cycles. P. 337-399. In: A.R. Robinson, J.J. McCarthy and B.J. Rothschild [eds], *The Sea*, Vol. 12, John Wiley and Sons.
- Gupta, G. V. M., Sudheesh, V., Sudharma, K.V., Saravanane, N., Dhanya, V., Dhanya, K.R., Lakshmi, G., Sudhakar, M., Naqvi, S.W.A., 2016. Evolution to decay of upwelling and associated biogeochemistry over the southeastern Arabian Sea shelf. *J. Geophys. Res.: Biogeosci.* 121, 159-175.
- Gupta, G.V.M., Jyothibabu, R., Ramu, C.V., Reddy, A.Y., Balachandran, K.K., Sudheesh, V., Kumar, S., Chari, N.V.H.K., Bepari, K.F., Marathe, P.H., Reddy, B.B., Vijayan, A.K., 2021. The world's largest coastal deoxygenation zone is not anthropogenically driven. *Environ. Res. Lett.* 16, 054009.
- Hannig, M., Lavik, G., Kuypers, M. M. M., Woebken, D., Martens-Habbena, W., Jürgens, K., 2007. Shift from denitrification to anammox after inflow events in the central Baltic Sea. *Limnol. Oceanogr.* 52(4): 1336-1345.
- Hietanen, S., Jantti, H., Buizert, C., Jürgens, K., Labrenz, M., Voss, M., Kuparinen, J., 2012. Hypoxia and nitrogen processing in the Baltic Sea water column. *Limnol. Oceanogr.* 57(1): 325-337.
- Holtappels, M., Lavik, G., Jensen, M. M., Kuypers, M. M. M., 2011. ^{15}N -Labelling experiments to dissect the contributions of heterotrophic denitrification and anammox to nitrogen removal in the OMZ waters of the ocean. *Methods Enzymol.* 486, 223-251.
- Holtermann, P.L., Umlauf, L., 2012. The Baltic Sea tracer release experiment: 2. Mixing processes. *J. Geophys. Res.* 117, C01022, doi:10.1029/2011JC007445, 2012.

- Howarth, R. W., 1988. Nutrient limitation of net primary production in marine ecosystems. *Ann. Rev. Ecol.* 19, 89-110.
- Hügler, M., Wirsén, C.O., Fuchs, G., Taylor, C.D., Sievert, S.M., 2005. Evidence for autotrophic CO₂ fixation via the reductive tricarboxylic acid cycle by members of the ϵ subdivision of proteobacteria. *J. Bacteriol.* 187 (9), 3020-3027.
- Ingole, B. S., Sautya, S., Sivadas, S., Singh, R., Nanajkar, M., 2010. Macrofaunal community structure in the western Indian continental margin including the oxygen minimum zone, *Mar. Ecol. Evol. Persp.* 31, 148–166.
- Jayakumar, D.A., Francis, C.A., Naqvi, S.W.A., Ward, B.B., 2004. Diversity of nitrite reductase genes (*nirS*) in the denitrifying water column of the coastal Arabian Sea. *Aquat. Microb. Ecol.* 34, 69-78.
- Jensen, M.M., Kuypers, M.M.M., Lavik, G., Thamdrup, B., 2008. Rates and regulation of anaerobic ammonium oxidation and denitrification in the Black Sea. *Limnol. Oceanogr.* 53(1), 23-36.
- Jensen M.M., Petersen, J., Dalsgaard, T., Thamdrup, B., 2009. Pathways, rates, and regulation of N₂ production in the chemocline of an anoxic basin, Mariager Fjord, Denmark. *Mar. Chem.* 113, 102-113.
- Joye, S., Hollibaugh, J. T., 1995. Influence of sulfide inhibition of nitrification on nitrogen regeneration in sediments, *Science* 270, 623–625.
- Kalvelage T., Lavik, G., Jensen, M.M., Revsbech, N.P., Löscher, C., Schunck, H., Desai, D.K., Hauss, H., Kiko, R., Holtappels, M., LaRoche, J., Schmitz, R.A., Graco M.I., Kuypers, M.M., 2015. Aerobic microbial respiration in oceanic oxygen minimum zones. *PLoS One* 10(7), e0133526. Doi:10.1371/journal.pone.0133526.
- Kamaleson, A.S., Gaosalves, M.J., Kumar, S., Jineesh, V.K., Lokabharathi, P.A., 2019. Spatio-temporal variations in sulfur-oxidizing and sulfate-reducing bacterial activities during upwelling, off south-west coast of India. *Oceanologia* 61, 427-444.
- Kartal, B., Kuypers, M.M.M., Lavik, G., Schalk, J., Op den Camp, H.J.M., Jetten, M.S.M., Strous, M., 2007. Anammox bacteria disguised as denitrifiers: nitrate reduction to dinitrogen gas via nitrite and ammonium. *Environ. Microbiol.* 9 (3), 635-642.
- Krishnan, K. P., Fernandes, S. O., Loka Bharathi, P. A., Krishna Kumari, L., Nair, S., Pratihary, A. K., Rao, B. R., 2008: Anoxia over the western continental shelf of India: Bacterial indications of intrinsic nitrification feeding denitrification, *Mar. Environ. Res.* 65, 445–455.
- Kuypers M. M. M., Sliemers, A.O., Lavik, G., Schmid, M., Jørgensen, B.B., Kuenen, J.G., Damste, J.S.S., Strous, M., Jetten, M.S.M., 2003. Anaerobic ammonium oxidation by anammox bacteria in the Black Sea. *Nature* 422, 608-611.
- Kuypers, M.M.M., Lavik, G., Woebken, D., Schmid, M., Fuchs, B. M., Amann, R., Jørgensen, B. B., Jetten, M. S. M., 2005. Massive nitrogen loss from the Benguela upwelling system through anaerobic ammonium oxidation. *Proc. Natl. Acad. Sci.* 102, 6478-6483.
- Lam, P., Lavik, G., Jensen, M.M., van de Vossenberg, J., Schmid, M., Woebken, D., Gutiérrez, D., Amann, R., Jetten, M.S.M., Kuypers, M.M.M., 2009. Revising the nitrogen cycle in the Peruvian oxygen minimum zone. *PNAS* 106 (12), 4752-4757.
- Lam, P., Kuypers, M. M. M., 2011. Microbial nitrogen cycling processes in oxygen minimum zones. *Annu. Rev. Mar. Sci.* 3, 317-345.
- Lass, H.U., Phrandke, H., Liljebladh, B. (2003). Dissipation in the Baltic proper during winter stratification. *J. Geophys. Res. (Ocean)* 108, doi:10.1029/2002JC001401.

- Lavik, G., Stuhmann, T., Brüchert, V., Van der Plas, A., Mohrholz, V., Lam, P., Musmann, M., Fuchs, B.M., Amann, R., Lass, U., Kuypers, M.M.M., 2009. Detoxification of sulphidic African shelf waters by blooming chemolithotrophs. *Nature* 457, 581–585.
- Levin L. A., Ekau, W., Gooday, A. J., Jorissen, F., Middelburg, J. J., Naqvi, S. W. A., Neira, C., Rabalais, N. N., Zhang, J., 2009. Effects of natural and human-induced hypoxia on coastal benthos. *Biogeosciences* 6, 2063-2098.
- Löscher C. R., Kock, A., Könneke, M., LaRoche, J., Bange, H. W., Schmitz, R.A., 2012. Production of oceanic nitrous oxide by ammonia-oxidizing archaea. *Biogeosciences* 9, 2419-2429.
- Louca, S., Hawley, A.K., Katsev, S., Torres-Beltran, M., Bhatia, M.P., Kheirandish, S., Michiels, C., Capelle, D., Lavik, G., Doebeli, M., Crowe, S.A., Hallam, S.J., 2016. Integrating biogeochemistry with multiomic sequence information in a model oxygen minimum zone. *PNAS* 113 (40), E5925-E5933.
- Mallik, T. K., 2008. *Marine Geology: A scenario around Indian coasts*, New Academic Publishers.
- Manning C. C., Hamme, R. C., Bourbonnais, A., 2010. Impact of deep-water renewal events on fixed nitrogen loss from seasonally-anoxic Saanich inlet. *Mar. Chem.* 122, 1-10.
- Marchant H. K., Ahmerkamp, S., Lavik, G., Tegetmeyer, H.E., Graf, J., Klatt, J.M., Holtappels, M., Walpersdorf, E., Kuypers, M.M.M., 2017. Denitrifying community in coastal sediments performs aerobic and anaerobic respiration simultaneously. *ISME J.* 11, 1799-1812.
- Marchant H. K., Tegetmeyer, H.E., Ahmerkamp, S., Holtappels, M., Lavik, G., Graf, J., Schreiber, F., Mussman, M., Strous, M., Kuypers, M.M.M., 2018. Metabolic specialization of denitrifiers in permeable sediments controls N₂O emissions. *Environ. Microbiol.* 20 (12), 4486-4502.
- McAuliffe, C., 1971. GC determination of solutes by multiple phase equilibration, *Chem. Technol.* 1, 46–50.
- Menezes, L., Fernandes, G.L., Mulla A.B., Meena R.M., Damare, S.R., 2020. Diversity of culturable sulphur-oxidising bacteria in the oxygen minimum zones of the northern Indian Ocean. *J. Mar. Syst.* 209, 103085.
- Michiels, C.C., Huggins, J.A., Giesbrecht, K.E., Spence, J.S., Simister, R.L., Varela, D.E., Hallam, S.J., Crowe, S.A., 2019. Rates and pathways of N₂ production in a persistently anoxic fjord: Saanich Inlet, British Columbia. *Front. Mar. Sci.* 6:27, doi: 10.3389/fmars.2019.00027.
- Millero, F.J., 1986. The thermodynamics and kinetics of the hydrogen sulphide system in natural waters. *Mar. Chem.* 81, 121-147.
- Montes E., Altabet, M.A., Muller-Karger, F.E., Scranton, M.I., Thunell, R.C., Benitez-Nelson, C., Lorenzoni, L., Astor, Y.M., 2013. Biogenic nitrogen gas production at the oxic-anoxic interface in the Cariaco basin, Venezuela. *Biogeosciences* 10,267-279.
- Nicholls, P., Kim, J.K., 1982. Sulfide as an inhibitor and electron donor for the cytochrome-c oxidase system. *Can. J. Biochem. Cell B* 60, 613-623.
- Naik, R., Naqvi, S.W.A., Araujo, J., 2016. Anaerobic carbon mineralization through sulphate reduction in the inner shelf sediments of eastern Arabian Sea. *Estuar. Coast.* 40, 134-144.
- Naik, V., Damare, S.R., Shah, S.S., Shenoy, D.M., Mulla, A.B., Coastal hypoxia drives microbial diversity: Elucidation through 16S rRNA amplicon sequencing. *Estuar.Coast. Shelf. Sci.* (Under review).
- Naqvi, S.W.A., Noronha, R.J., 1991. Nitrous oxide in the Arabian Sea. *Deep-Sea Res.* 38 (7), 871-890.

Naqvi, S.W. A., Jayakumar, D. A., Narvekar, P. V., Naik, H., Sarma, V. V. S. S., D'Souza, W., Joseph, S., George, M. D., 2000. Increased marine production of N₂O due to intensifying anoxia on the Indian continental shelf. *Nature*, 408, 346–349.

Naqvi, S. W. A., H. Naik, D. A. Jayakumar, M. S. Shailaja, and P. V. Narvekar. 2006. Seasonal oxygen deficiency over the western continental shelf of India, p. 195–224. In L. N. Neretin [ed.], *Past and Present Water Column Anoxia*. Springer.

Naqvi, S.W.A., Naik, H., Jayakumar, A., Pratihary, A.K., Narvekar, G., Kurian S., Agnihotri, R., Shailaja, M.S., Narvekar, P.V., 2009. Seasonal anoxia over the Western Indian continental shelf. In: Wiggert, J.D., Hood, R.R., Naqvi, S.W.A., Brink, K.H., Smith, S.L. (Eds.), *Indian Ocean biogeochemical processes and ecological variability*, Geophysical Monograph Series, Vol. 185, American Geophysical Union, pp. 333-345.

Naqvi, S.W.A., Bange, H.W., Farias, L., Monteiro, P.M.S., Scranton, M.I., Zhang, J., 2010. Marine hypoxia/anoxia as a source of CH₄ and N₂O. *Biogeosciences* 7, 2159-2190.

Ohde, T., 2018. Coastal sulfur plumes off Peru during El Nino, La Nina, and neutral phases. *Geophys. Res. Lett.* 45, <https://doi.org/10.1029/2018GL077618>.

Ohde, T., Dadou, I., 2018. Seasonal and annual variability of coastal sulphur plumes in the northern Benguela upwelling system. *PLoS ONE* 13 (2), e0192140. <https://doi.org/10.1371/journal.pone.0192140>.

Otte S., Grobden, N.G., Robertson, L.A., Jetten, M.S.M., Kuenen, J. G., 1996. Nitrous oxide production by *Alcaligenes faecalis* under transient and dynamic aerobic and anaerobic conditions. *Appl. Environ. Microbiol.* 62 (7): 2421-2426.

Petersen, L.C., 1977. Effect of inhibitors on oxygen kinetics of cytochrome-c oxidase. *Biochim. Biophys. Acta* 460, 299-307.

Parvathi, V., Suresh, I., Langaigane, M., Ethe, C., Vialard, J., Levy, M., Neetu, S., Aumont, O., Resplandy, L., Naik, H., Naqvi, W., 2017. Positive Indian Ocean Dipole events prevents anoxia off the west coast of India. *Biogeosciences*, 14, 1541-1559.

Pitcher, G.C., Aguirre-Velarde, A., Breitburg, D., Cardich, J., Carstensen, J., Conley, D.J., Dewitte, B., Engel, A., Espinoza-Morriberón, D., Flores, G., Garçon, V., Graco, M., Grégoire, M., Gutiérrez, D., Hernandez-Ayon, J.M., Huang, H.M., Isensee, K., Jacinto, M.E., Levin, L., Lorenzo, A., Machu, E., Merma, L., Montes, I., Naqvi, S.W.A., Paulmier, A., Roman, M., Rose, K., Hood, R., Rabalais, N.N., Salvanes, A.G., Salvatecci, R., Sánchez, S., Sifeddine, A., Tall, A.W., van der Plas, A.K., Yasuhara, M., Zhang, J., Zhu, Z., 2021. System controls of coastal and open ocean oxygen depletion. *Prog. Oceanogr.* 197, 102613.

Pratihary, A.K., Naqvi, S.W.A., Narvenkar, G., Kurian, S., Naik, H., Naik, R., Manjuanatha, B.R., 2014. Benthic mineralization and nutrient exchange over the inner continental shelf of western India. *Biogeosciences* 11, 2771-2791.

Preisler, A., de Beer, D., Lichtschlag, A., Lavik, G., Boetius, A., Jørgensen, B. B., 2007. Biological and chemical oxidation in a *Beggiatoa* inhabited marine sediment. *ISME J.* 1, 341-353.

Rao, A.D., Joshi, M., Ravichandran, M., 2008. Oceanic upwelling and downwelling processes in waters off the west coast of India. *Ocean Dynamics* 58, 213-226.

Richards, F.A., Cline, J.D., Broenkow, W.W., Atkinson, L.P., 1965. Some consequences of the decomposition of organic matter in Lake Nitinat, an anoxic fjord. *Limnol. Oceanogr.* 10, R185-R201.

Robertson, L.A., Kuenen, J.G., 2006. The Genus *Thiobacillus*. *Prokaryotes* 5, 812-827.

- Sarkar A., Naqvi, S. W. A., Lavik, G., Pratihary, A., Naik, H., Shirodkar, G., Kuypers M. M. M., 2020. Massive nitrogen loss over the western Indian continental shelf during seasonal anoxia: Evidence from isotope pairing technique. *Front. Mar. Sci.* 7: 1-14.
- Schulz, H. D., 2006. Quantification of early diagenesis: Dissolved constituents in pore water and signals in the solid phase, p. 73–124. In H.D. Schulz and M. Zabel [eds.], *Marine Geochemistry*. Springer.
- Schunk, H., Lavik, G., Deasi, D.K., Großkopf, T., Kalvelage, T., Loscher C.R., Paulmier, A., Contreras, S., Siegel, H., Holtappels, M., Rosenstiel, P., Schilhabel, M.B., Graco, M., Schmitz, R.A., Kuypers, M.M.M., LaRoache, J., 2013. Giant hydrogen sulphide plume in the oxygen minimum zone off Peru supports chemolithoautotrophy. *PLoS One* 8, 1-18.
- Senga, Y., Mochida, K., Fukumori, R., Okamoto, N., Seike, Y., 2006. N₂O accumulation in estuarine and coastal sediments: The influence of H₂S on dissimilatory nitrate reduction. *Estuar. Coast. Shelf Sci.* 67: 231-238.
- Shao, M.F., Zhang, T., Fang, H.P., 2010. Sulfur-driven autotrophic denitrification: diversity, biochemistry, and engineering applications. *Appl. Microbiol. Biotechnol.* 88, 1027-1042.
- Shenoi, S., Antony, M.K., 1991. Current measurements over the western continental shelf of India. *Cont. Shelf Res.* 11 (1), 81-93.
- Shenoy, D.M., Sujith, K.B., Guans, M.U., Patil, S., Sarkar A., Naik, H., Narvekar, P.V., Naqvi, S.W.A., 2012. Production of dimethylsulphide during the seasonal anoxia off Goa. *Biogeochemistry* 110, 47-55.
- Shirodkar, G., Naqvi, S.W.A., Naik, H., Pratihry, A.K., Kurian, S., Shenoy, D.M., 2018. Methane dynamics in the shelf waters of the West coast of India during seasonal anoxia. *Mar. Chem.* 203, 55-63.
- Song, G. D., Liu, S. M., Kuypers, M. M. M., Lavik, G., 2016. Application of the isotope pairing technique in sediments where anammox, denitrification and dissimilatory nitrate reduction to ammonium coexist. *Limnol. Oceanogr.: Methods* 14: 801-815.
- Sørensen, J., Tiedje, J.M., Firestone R.B., 1980. Inhibition of sulfide of nitric and nitrous oxide reduction by denitrifying *Pseudomonas fluorescens*. *Appl. Environ. Microbiol.* 39 (1), 105-108.
- Stramma, L., Johnson, G.C., Sprintall, J., Mohrholz, V., 2008. Expanding oxygen minimum zones in the tropical oceans. *Science* 320, 655-658.
- Sullivan, M.J., Gates, A.J., Appia-Ayme. C., Rowley, G., Richardson, D.J., 2013. Copper control of bacterial nitrous oxide emission and its impact on vitamin B₁₂-dependent metabolism. *PNAS* 110, 19926- 19931.
- Suter, E.A., Pachiadaki, M.G., Montes, E., Edgcomb, V.P., Scranton, M.I., Taylor, C.D., Taylor, G.T., 2021. Diverse nitrogen cycling pathways across a marine oxygen gradient indicate nitrogen loss coupled to chemoautotrophic activity. *Environ. Microbiol.* 23(6), 2747-2764.
- Taylor, G.T., Iabichella, M., Ho, T.Y., Scranton, M.I., Thunell, R.C., Muller-Karger, F., Varela, R., 2001. Chemoautotrophy in the redox transition zone of the Cariaco Basin: A significant midwater source of organic carbon production. *Limnol. Oceanogr.* 46 (1), 148-163.
- Thamdrup, B., Dalsgaard, T., Jensen, M. M., Ulloa, O., Farias, L., Escobedo, R., 2006. Anaerobic ammonium oxidation in the oxygen-deficient waters off northern Chile. *Limnol. Oceanogr.* 51(5), 2145-2156.
- Tyrrell, T., 1999. The relative influences of nitrogen and phosphorus on oceanic primary production. *Nature* 400, 525-531.

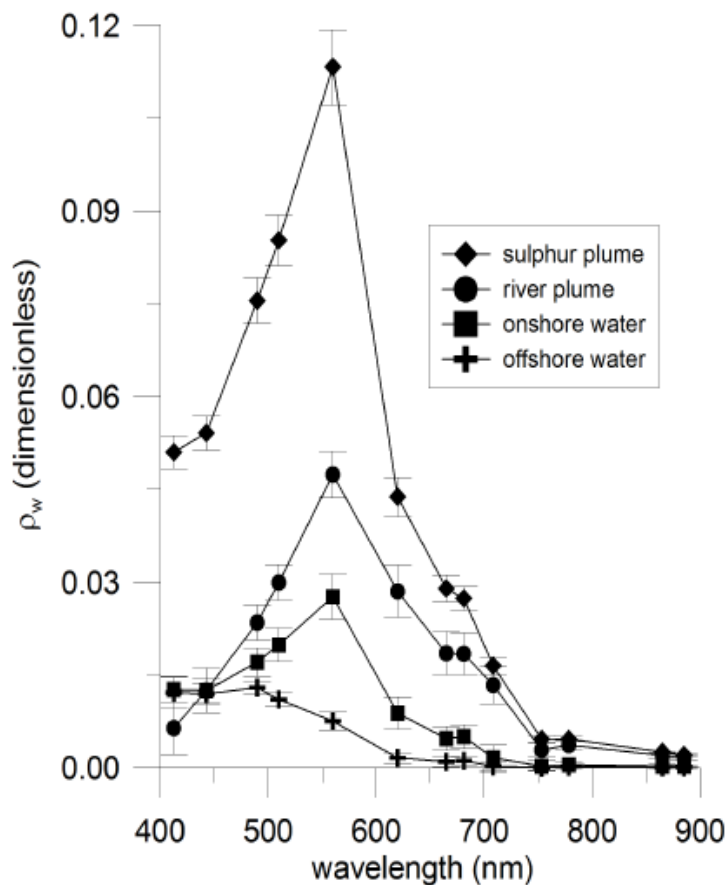
- Unnikrishnan, A.S., Antony, M.K., 1990. On the vertical velocity fluctuations and internal tides in an upwelling region of the West coast of India. *Estuar. Coast. Shelf Sci.* 31, 865-873.
- Van Vliet, D.M., von Meijenfildt, F.A.B., Dutilh, B.E., Sinnige-Damsté, J.S., Stams, J.M., Sánchez-Andrea I., 2020. The bacterial sulfur cycle in expanding dysoxic and euxinic marine waters. *Environ. Microbiol.* 23(6), 2834-2857.
- Vaquer-Sunyer, R., Duarte, C. M., 2010. Sulfide exposure accelerates hypoxia-driven mortality. *Limnol. Oceanogr.* 55(3), 1075-1082.
- Ward, B.B., Tuit, C.B., Jayakumar, A., Rich, J.J., Moffett, J., Naqvi, S.W.A., 2008. Organic carbon, and not copper, controls denitrification in oxygen minimum zones of the ocean. *Deep-Sea Res. I* 55, 1672-1683.
- Warembourg, F. R., 1993. Nitrogen fixation in soil and plant systems, p. 127-156. In R. Knowles, E. A. Paul, J. Melillo and H. Blackburn [eds.], *Nitrogen Isotope Techniques*. Academic Press.
- Walsh, D. A., Zaikova, E., Howes, C. G., Song, Y. C., Wright, J. J., Tringe, S. G., Tortell, P. D., Hallam, S. J., 2009. Metagenome of a versatile chemolithoautotroph from expanding oceanic dead zones. *Science* 326, 578-582.
- Xi Q., Babbin, A., Jayakumar, A., Oleynik, S., Ward, B.B., 2015. Nitrous oxide production by nitrification and denitrification in the Eastern Tropical South Pacific oxygen minimum zone. *Geophys. Res. Lett.* 42, 10,755–10,764, doi:10.1002/2015GL066853.
- Zaikova, E., Walsh, D. A., Stilwell, C. P., Mohn, W. W., Tortell, P. D., Hallam, S. J., 2010. Microbial community dynamics in a seasonally anoxic fjord: Saanich Inlet, British Columbia. *Environ. Microbiol.* 12, 172-191.
- Zopfi, J., Ferdelman, T. G., Jørgensen, B. B., Teske, A., Thamdrup, B., 2001. Influence of water column dynamics on sulphide oxidation and other major biogeochemical processes in the chemocline of Mariager Fjord (Denmark). *Mar. Chem.* 74, 29-51

Supplementary materials

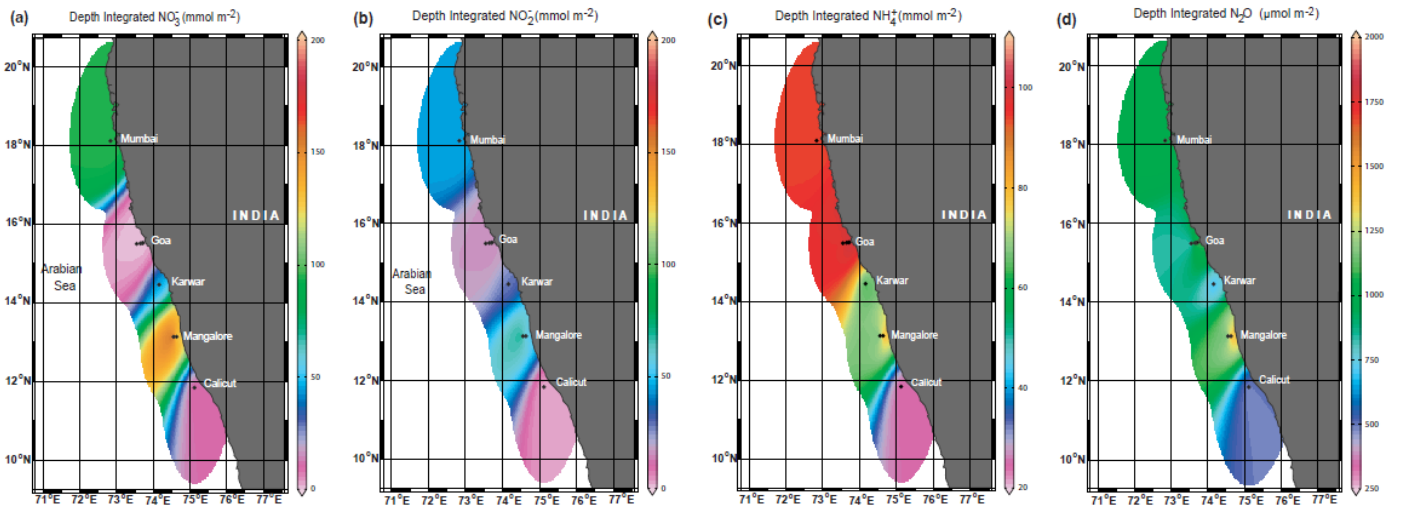
Detection of the elemental sulphur plume over the WICS through satellite imagery

During the observation period of 15 September to 7 October 2011, a large plume of colloidal elemental sulphur (S^0) was observed in the surface waters between $11.5^\circ\text{N} - 11.8^\circ\text{N}$ and $75.2^\circ\text{E} - 75.3^\circ\text{E}$, an area located between the Mangalore and Calicut transects. The formation of colloidal sulphur can be only observed under special conditions such as upwelling and anoxic events. Sulphur plume could well be quite frequent during the late summer monsoon when the sulphidic events occur but could be largely overlooked due to the high cloud coverage. Despite extensive cloud cover during the monsoon period, this event was visible in different MODIS and MERIS scenes between 18 and 21 September 2011 (Fig. 3). The size of the milky-turquoise patch covered approximately 700 km^2 of the shelf area. The innershelf area where the sulphide concentrations were detected had surface waters that exhibited the characteristics of river plume water, which likely prevented the upwelling of the sulphide/sulphur to the surface waters. However, the offshore shift in the sulphur patch compared to the sulphidic waters indicated that there is an offshore transport of the sulphidic waters from the shelf towards the open ocean.

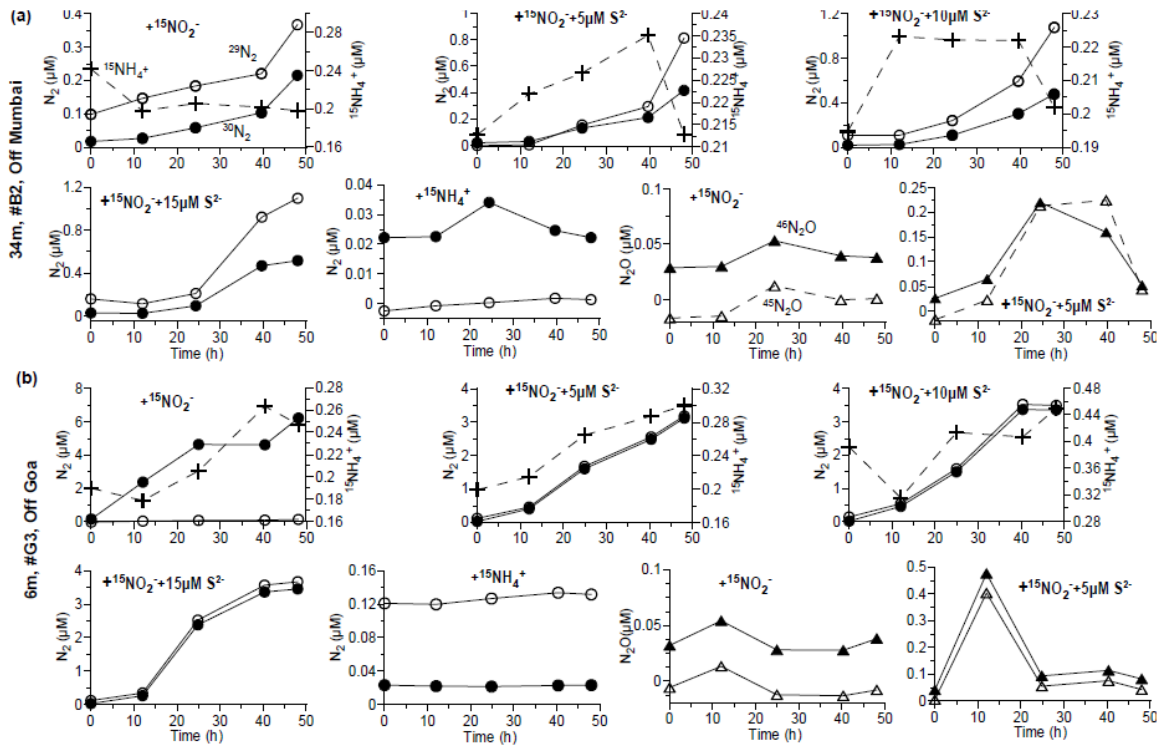
Supplementary Figures



Suppl Fig.1. Spectral signatures of sulphur plume, river plume, onshore water and offshore water on MERIS Bands off western India during September-October 2011.

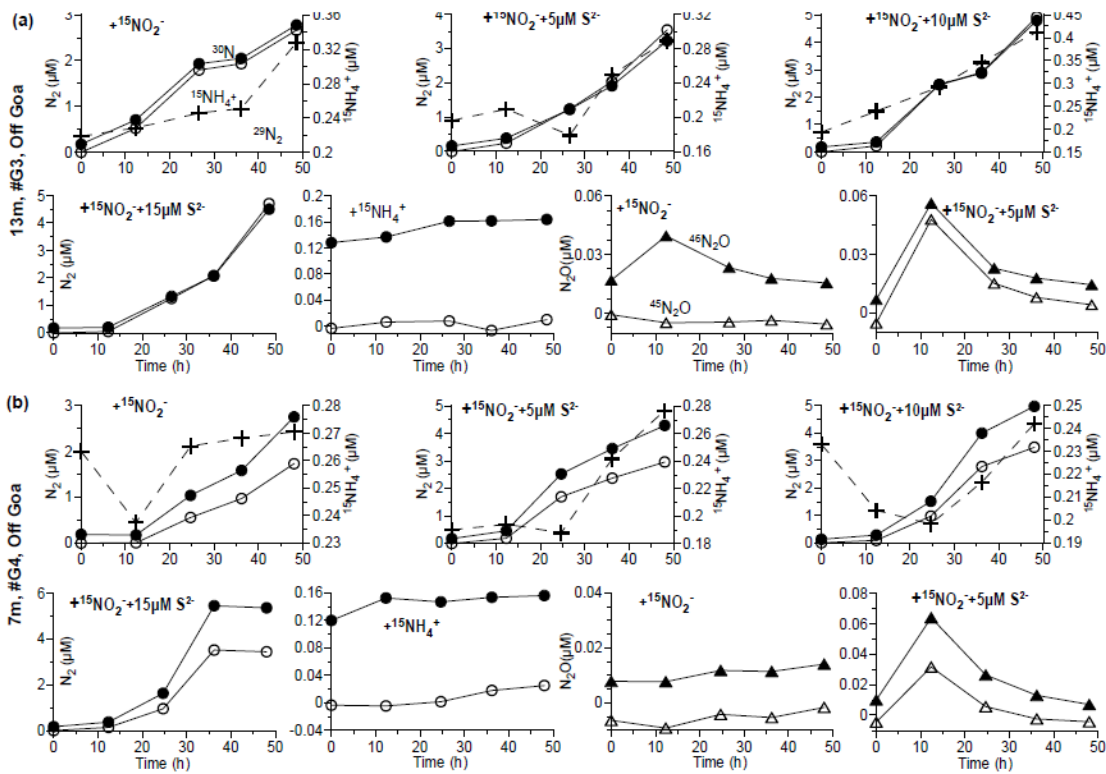


Suppl Fig. 2. Spatial variability of depth-integrated N-nutrients and N_2O along the innershelf of Western India during late SW monsoon.

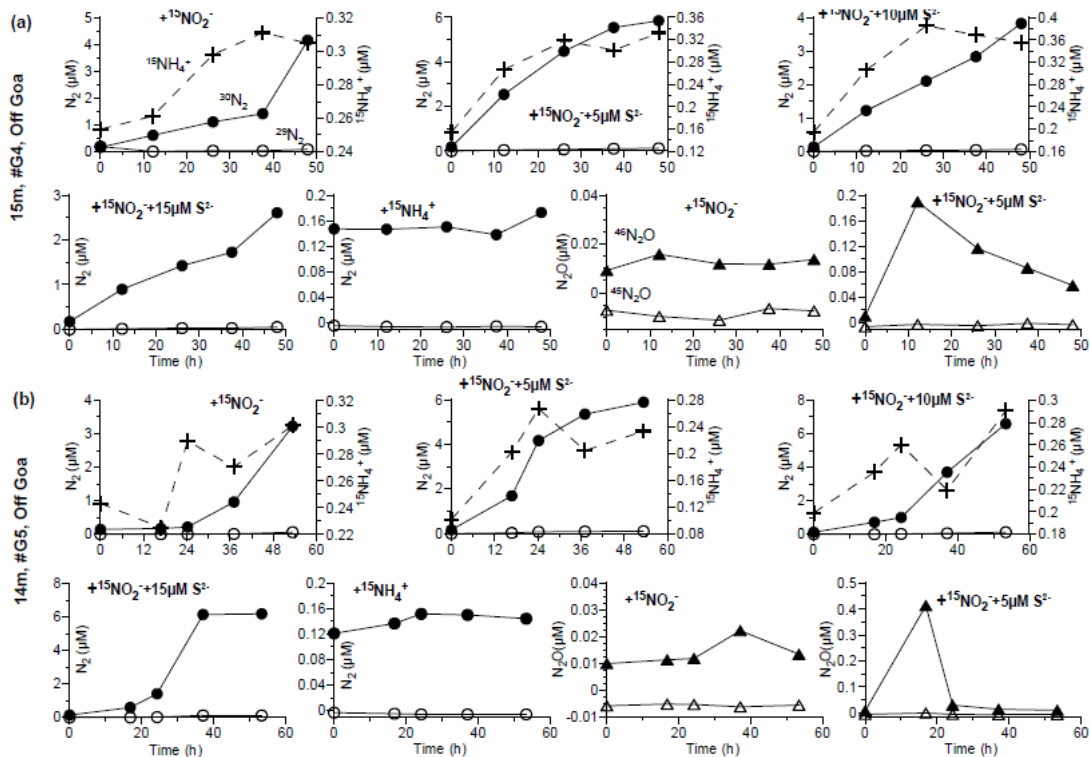


Suppl. fig. 3. Production of $^{15}N-N_2$, $^{15}NH_4^+$ and $^{15}N-N_2O$ from ^{15}N -incubations at 34m, B2 (off Mumbai) and 6m, G3 (off Goa).

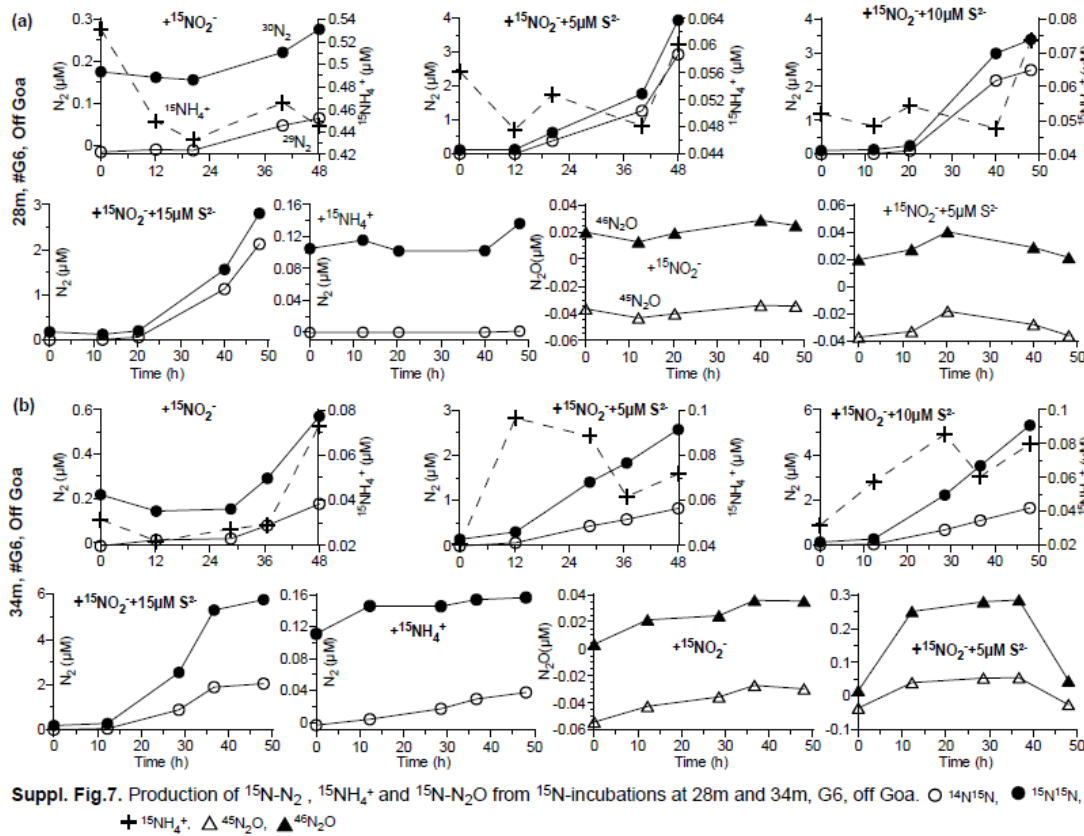
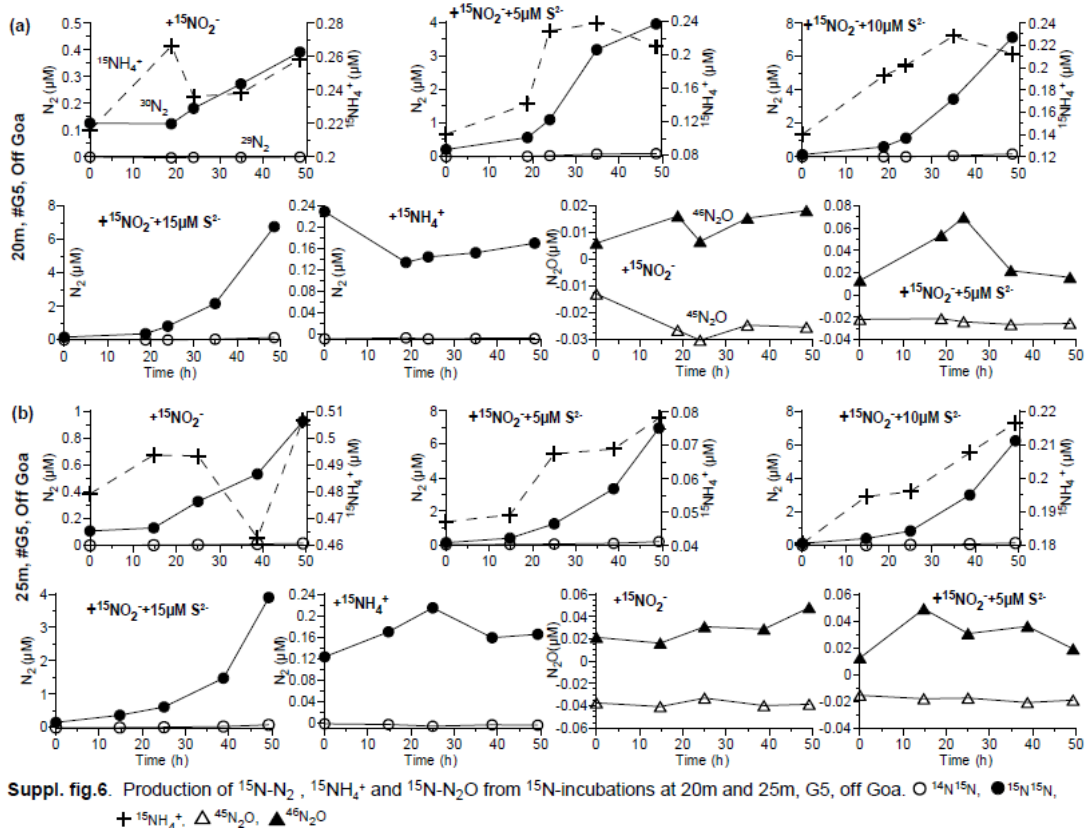
○ $^{14}N^{15}N$, ● $^{15}N^{15}N$, + $^{15}NH_4^+$, △ $^{45}N_2O$, ▲ $^{46}N_2O$.

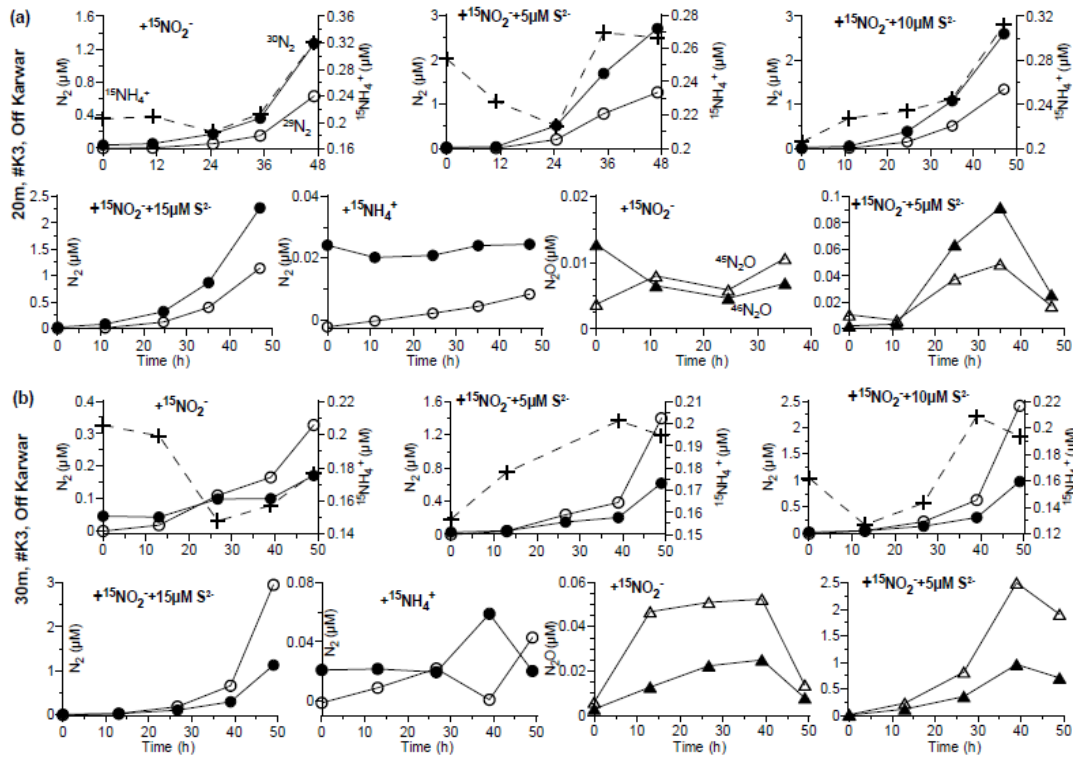


Suppl. fig. 4. Production of $^{15}\text{N-N}_2$, $^{15}\text{NH}_4^+$ and $^{15}\text{N-N}_2\text{O}$ from ^{15}N -incubations at 13m, G3 and 7m, G4, off Goa. \circ $^{14}\text{N}^{15}\text{N}$, \bullet $^{15}\text{N}^{15}\text{N}$, $+$ $^{15}\text{NH}_4^+$, \triangle $^{45}\text{N}_2\text{O}$, \blacktriangle $^{46}\text{N}_2\text{O}$

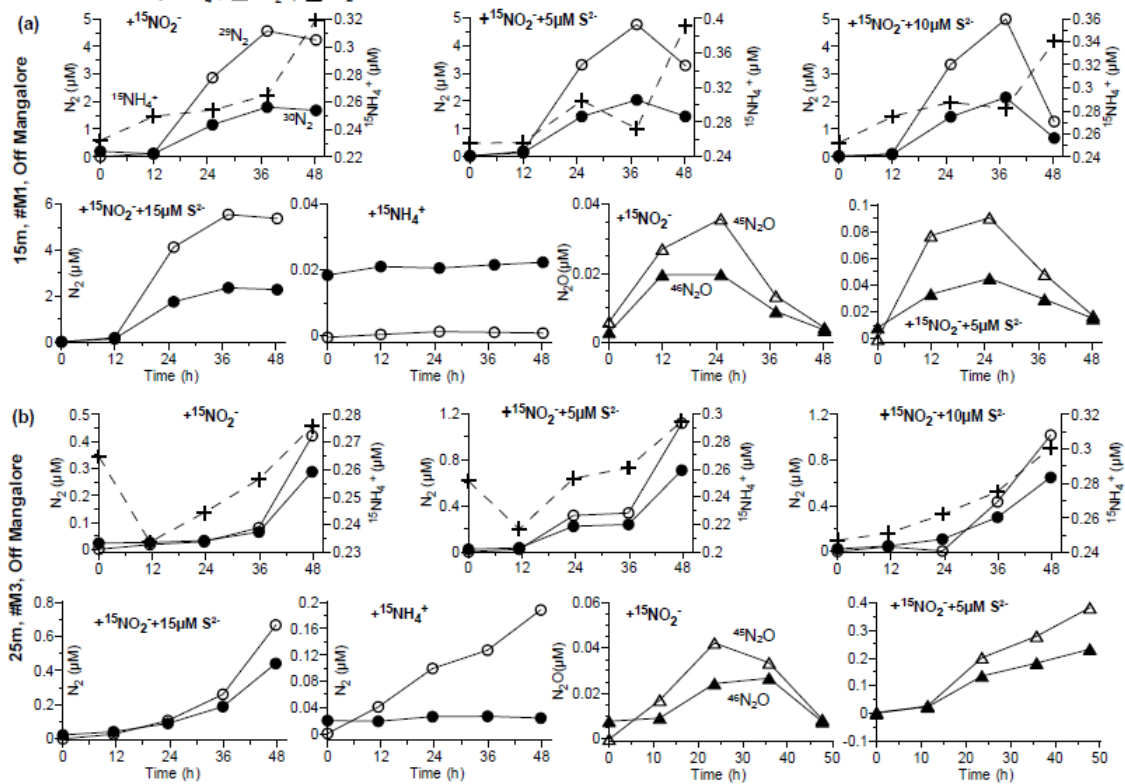


Suppl. fig. 5. Production of $^{15}\text{N-N}_2$, $^{15}\text{NH}_4^+$ and $^{15}\text{N-N}_2\text{O}$ from ^{15}N -incubations at 15m, G4 and 14m, G5, off Goa. \circ $^{14}\text{N}^{15}\text{N}$, \bullet $^{15}\text{N}^{15}\text{N}$, $+$ $^{15}\text{NH}_4^+$, \triangle $^{45}\text{N}_2\text{O}$, \blacktriangle $^{46}\text{N}_2\text{O}$

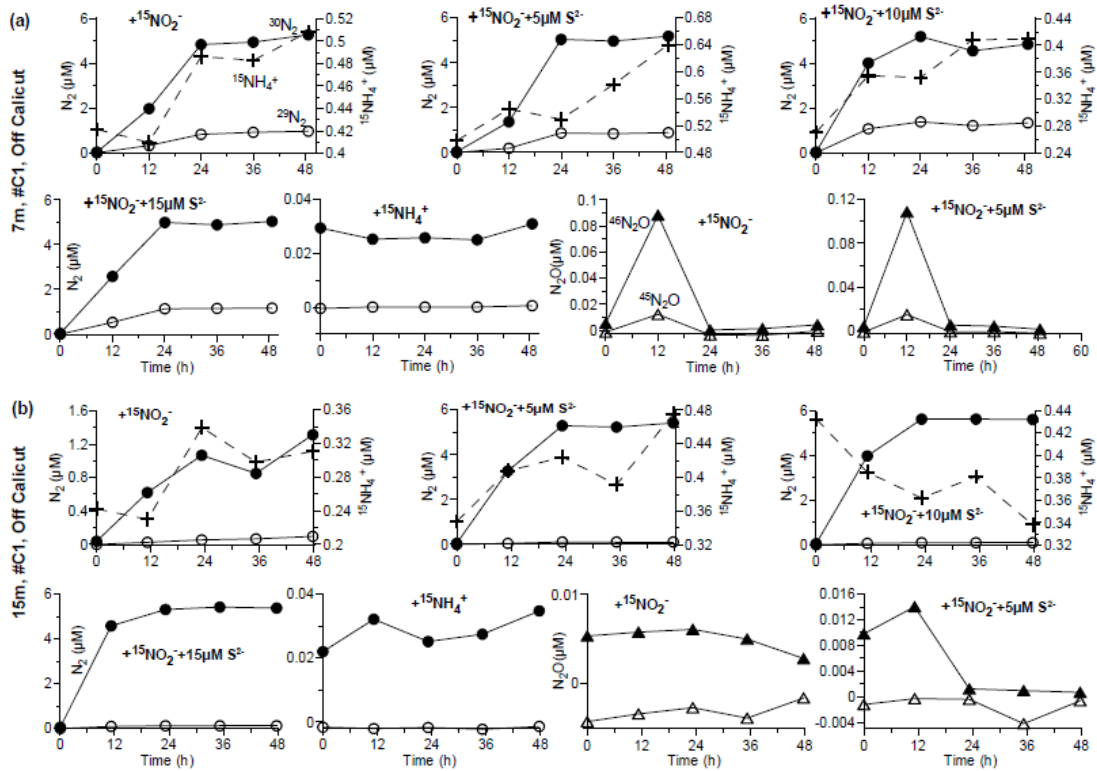




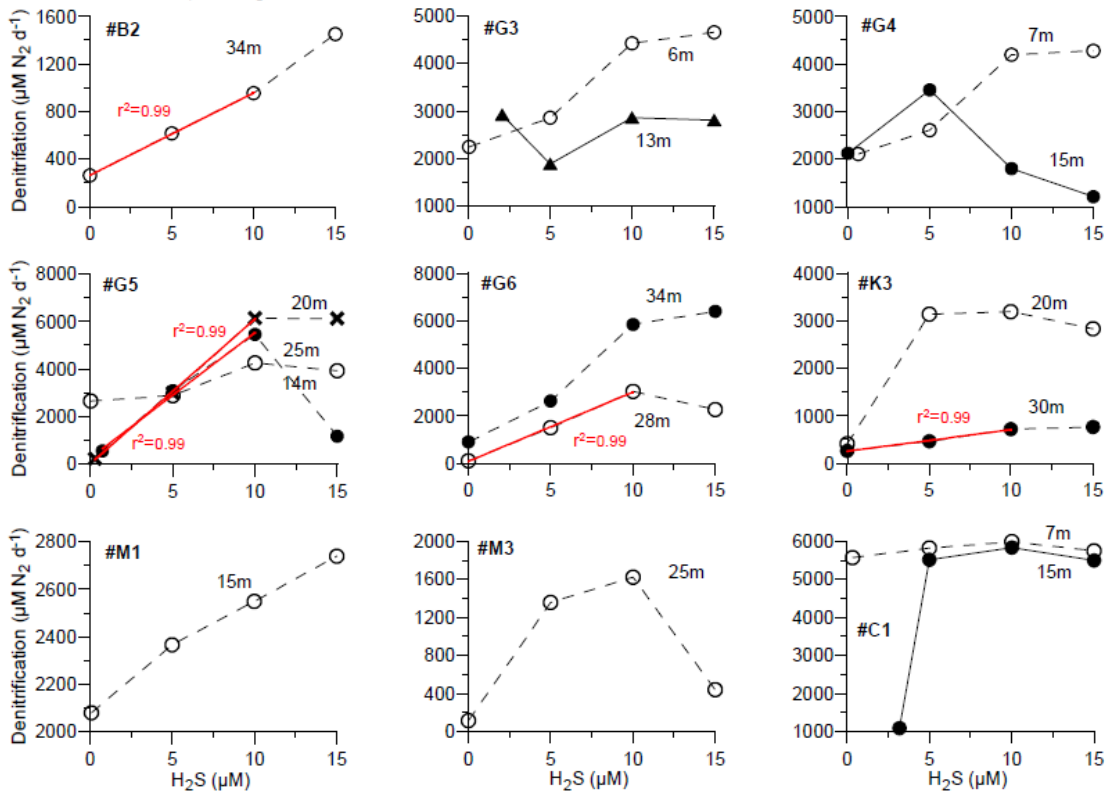
Suppl. Fig.8. Production of $^{15}\text{N-N}_2$, $^{15}\text{NH}_4^+$ and $^{15}\text{N-N}_2\text{O}$ from ^{15}N -incubations at 20m and 30m, K3, off Karwar. \circ $^{14}\text{N}^{15}\text{N}$, \bullet $^{15}\text{N}^{15}\text{N}$, $+$ $^{15}\text{NH}_4^+$, \triangle $^{45}\text{N}_2\text{O}$, \blacktriangle $^{46}\text{N}_2\text{O}$



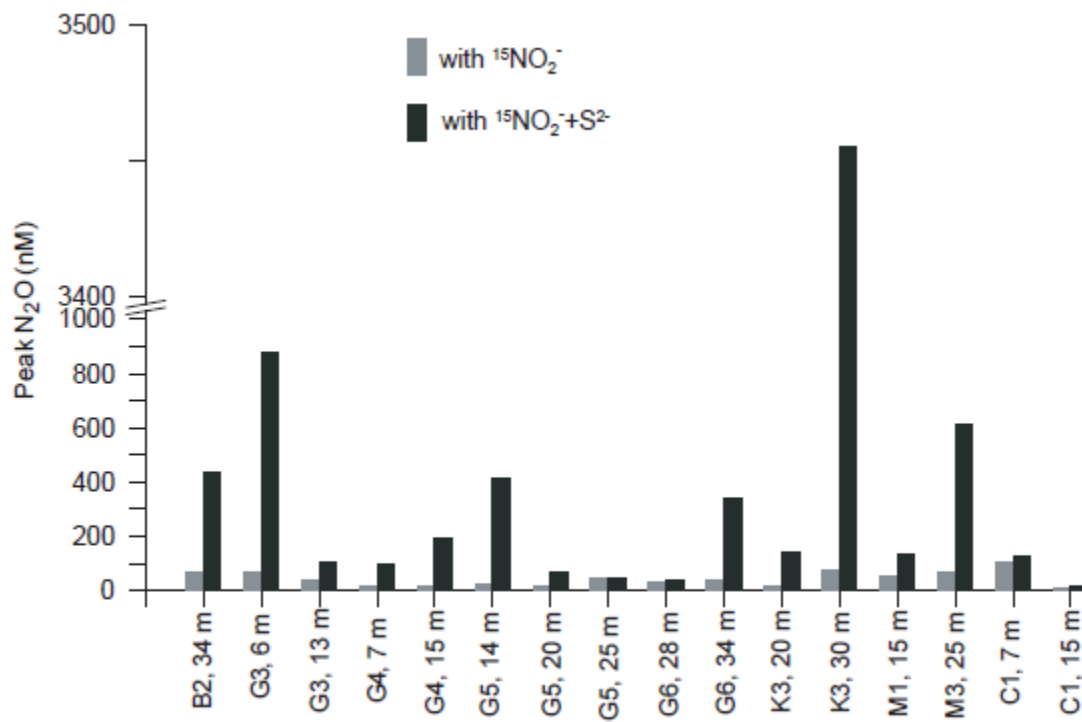
Suppl. Fig.9. Production of $^{15}\text{N-N}_2$, $^{15}\text{NH}_4^+$ and $^{15}\text{N-N}_2\text{O}$ from ^{15}N -incubations at 15m, #M1 and 25m, #M3, off Mangalore. \circ $^{14}\text{N}^{15}\text{N}$, \bullet $^{15}\text{N}^{15}\text{N}$, $+$ $^{15}\text{NH}_4^+$, \triangle $^{45}\text{N}_2\text{O}$, \blacktriangle $^{46}\text{N}_2\text{O}$



Suppl. Fig.10. Production of $^{15}\text{N-N}_2$, $^{15}\text{NH}_4^+$ and $^{15}\text{N-N}_2\text{O}$ from ^{15}N -incubations at 7m and 15m, #C1, off Calicut. \circ $^{14}\text{N}^{15}\text{N}$, \bullet $^{15}\text{N}^{15}\text{N}$, $+$ $^{15}\text{NH}_4^+$, \triangle $^{45}\text{N}_2\text{O}$, \blacktriangle $^{46}\text{N}_2\text{O}$



Suppl. Fig.11. Correlation of denitrification rates with sulphide concentration.



Suppl. Fig. 12. Peak N_2O concentration in the incubations with added $^{15}NO_2^-$ and $^{15}NO_2^- + S^{2-}$.